Gelatin Methacrylate as a Controlled Release Vehicle for Treatment of Recurrent Corneal Erosion

By

John Tse

A thesis

presented to the University of Waterloo

in fulfillment of the

thesis requirement for the degree of

Master of Applied Science

in

Chemical Engineering – Nanotechnology

Waterloo, Ontario, Canada, 2018

Author’s declaration

I hereby declare that I am the sole author of this thesis. This is a true copy of the thesis, including any required final revisions, as accepted by my examiners.

I understand that my thesis may be made electronically available to the public.

Abstract

Patients with recurrent corneal erosions (RCE) experience unpredictable and painful episodes, caused by the loss of superficial corneal epithelial cells. The erratic nature of RCE often leads to patient anxiety, and can significantly impact one's productivity and quality of life. Historically, patching (to prevent blinking) and ocular lubricants were the standard treatment for RCE. More recently, soft bandage contact lenses (BCLs) are commonly used, as this allows the use of vision during the healing process. The issue with BCLs is that they do not outperform ocular lubricants in terms of their efficacy or speed of recovery because they currently lack the biological factors that are crucial to ocular surface repair. Furthermore, ocular lubricants only possess a 5% bioavailability, with the majority of active ingredients being washed away by the tear film. Other treatments may involve more invasive methods such as anterior stromal puncture or phototherapeutic keratectomy which enhances the epithelial adhesion to Bowman's membrane or the underlying stroma.

The objective of this project was to fabricate and characterize gelatin methacrylate (GelMA) as an enzyme-triggered controlled release vehicle in the presence of matrix metalloproteinase (MMP) for either bovine lactoferrin (BLf) or hyaluronic acid (HA) and to test these molecules as viable drugs for enhancing corneal epithelial wound healing. GelMA revealed a tunable profile fit for diffusion- and enzyme-mediated controlled release of drugs above the 70kDa molecular weight range. A 70kDa FITC-dextran model molecule validated the effect of concentration of GelMA, methacrylation degree and UV irradiation on the controlled release profile. An increase in concentration and methacrylation degree resulted in a stronger and denser gel with a lower burst release, whereas a high UV irradiation dosage allowed for higher crosslinking. The incorporation of GelMA into a commercial Biofinity contact lens did not show significant change in the mechanical properties, light transmittance or water contact angle demonstrating promise for future applications. Although a GelMA-incorporated lens could not load an adequate amount of drug for the molecules selected, optimization through freeze-drying proved to increase loading by nearly 50%.

BLf demonstrated accelerated wound healing on the rabbit corneal epithelial scratch wound assay, whereas HA increased wound healing on both rabbit and human corneal epithelial cells in a scratch

and polydimethylsiloxane (PDMS) stamp wound model. The PDMS stamp wound assay provided a more consistent initial wound area and was used for future experiments. Similarly, HA was established to be more versatile in wound healing and was selected as the drug of focus.

The 60kDa HA-loaded GelMA patches showed promise in healing human corneal epithelial wounds at lower drug loadings of $150\mu g$ and $250\mu g$, however, the hydrogel became opaque after crosslinking. ELISA tests on the controlled release of HA-loaded GelMA confirmed that FITC-dextran was viable as a model molecule to reproduce release profiles.

Acknowledgements

I would like to express my gratitude to my supervisor, Dr Evelyn K.F. Yim, for her outstanding patience and regulated guidance throughout my Masters of Applied Science program. She has demonstrated endless support no matter what decisions I have made and has been encouraging every step of the way.

I am also indebted to my colleagues at the Regenerative Nanomedicine Lab, for their support and contribution to enabling my experiments to be performed smoothly and successfully. Sincere thanks to Dr. Muhammad Rizwan for his guidance and words of wisdom.

Last but not least, I would like to thank my family and friends, who have supported me through the course of my studies here at the University of Waterloo.

Table of Contents

List of Figures

List of Tables

List of Abbreviations (Alphabetical)

ANOVA	Analysis of variance
BCL	Bandage contact lens
BLf	Bovine Lactoferrin
CL	Contact Lens
ELISA	Enzyme linked immunosorbent assay
EpCM	Epithelial cell medium
FBS	Fetal bovine serum
FDA	Food and Drug Administration
FITC	Fluorescein isothiocyanate
GAG	Glycoasminoglycan
GelA	Gelatin type A
GelMA	Gelatin Methacrylate
GRAS	Generally recognized as safe
HA	Hyaluronic Acid
HCEpCs	Human corneal epithelial cells
KGS	Keratinocyte growth serum
KM	Keratinocyte media
MA	Methacrylic anhydride
MMP	Matrix metallopeptidase
PET	Polyethylene terephthalate
PI	Photoinitiator
P/S	Penicillin/Streptomycin
RCE	Recurrent corneal erosion
RCEpCs	Rabbit corneal epithelial cells
UV	Ultraviolet

1.0 Introduction

The eye is a vital organ that is responsible for one of five primary senses. It can be divided into two components: the anterior and posterior section. The cornea is a clear tissue that shields the front of the eye and is responsible for 70% of its refractive power [1]. Instead of receiving nutrients from blood like most tissues, the cornea obtains its nourishments from a tear that also serves as a protective layer to the cornea from the external environment [2].

There are several ways the cornea can be compromised. Common causes of injury may include physical abrasions, chemical wounds, incorrect contact lens fitting, introduction of foreign agents, or exposure to ultraviolet (UV) rays [3]. Physical abrasions can occur from rubbing one's eye too aggressively, whereas chemical wounds may originate from fluid entering the eye, such as an acidic beverage or a harsh cleaning substance. It is important that users of contact lenses follow the protocol given by the optometrist to avoid injury, as poor lens fitting or misuse of contact lens cleaning solution may cause corneal injuries. Foreign materials such as dust or sand may cause further damage and, on occasion, can penetrate beyond the corneal layer, causing severe damage [2]. Lastly, the cornea is susceptible everyday to the UV lights coming from sunlight, lamps, and even snow or water reflections [3].

All the aforementioned causes of injuries may lead to further eye-related complications such as recurrent corneal erosion (RCE). Although several treatment options are available to help heal RCE, the therapies are quite intensive and are not always effective. There is currently a need for a more efficient, user friendly, and commercially available remedy. We propose to investigate the use of a controlled release drug-loaded transparent hydrogel in improving RCE.

1.1 The Cornea

The cornea is a complex tissue composed of numerous layers of cells, each a specific function as illustrated in Figure 1. Beginning from the outer (anterior) to the inner (posterior) portion, the cornea is composed of the epithelium, Bowman's membrane, stroma, Descemet's membrane and the endothelium.

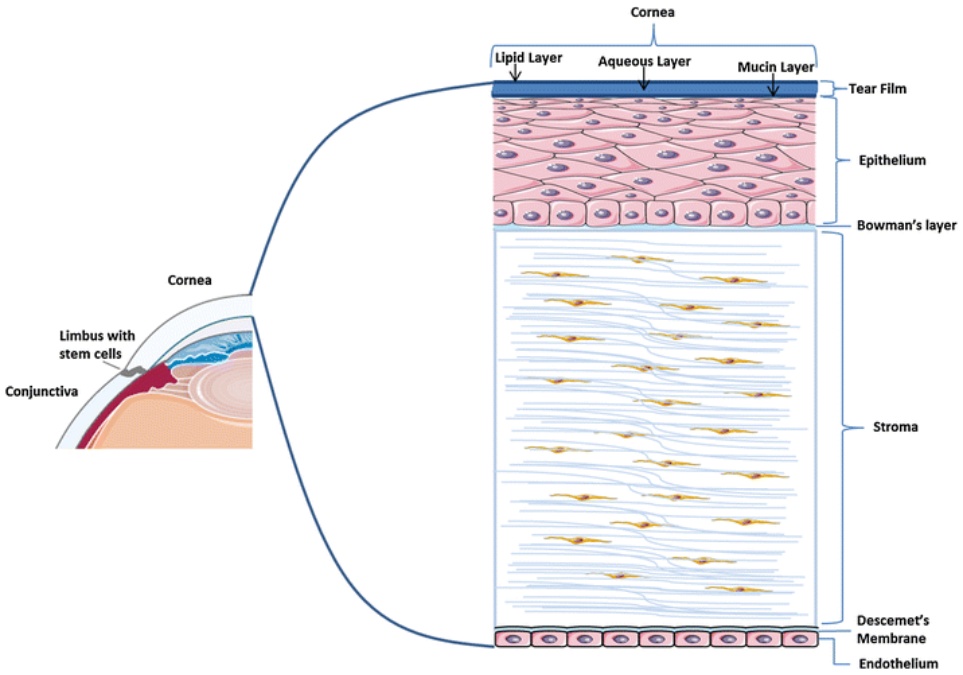

Figure 1. Structure of cornea including tear film[4]

The epithelium is comprised of several layers of corneal epithelial cells which are responsible for controlling a passageway into the eye. These cells prevent foreign bodies from entering, and provide a smooth surface to allow absorption of oxygen and nutrients from the tear film. The epithelium is also packed with nerve endings to alert the body of corneal injury, thereby providing a rapid response system [5].

The Bowman's membrane is a film of tissue composed primarily of collagen protein fibers and is the primary adhesion point for the corneal epithelium. The function of the Bowman's membrane, aside from securing the epithelial cells, is not quite clear, however, upon injury, the Bowman's membrane may scar during the healing process causing a loss of vision [6].

As this project primarily deals with the corneal epithelium, and its underlying membrane, the other portions of the cornea will not be discussed.

1.2 Tear Film

While not actually part of the cornea, the tear film is an essential component to keeping the eye hydrated and healthy, while additionally accelerating wound healing and preventing infection. The tear film is composed of a lipid, aqueous and mucin layer which are secreted by the Meibomian

gland, lacrimal gland and globlet cells, respectively [7] as seen in Figure 1. The lipid layer is the outermost level of the tear film and prevents the tears from evaporating too rapidly. The aqueous layer, in combination with the mucin layer, spread over the cornea to efficiently deliver nutrients to the eye.

The tear film is constantly being replenished on the eye to remove foreign compounds and to maintain a continuous flow of nutrition [8]. While this is advantageous to daily maintenance and overall healthiness of the eye, the constant flushing of the tear film renders delivering drugs difficult.

1.3 Recurrent Corneal Erosion

Having direct contact to the surrounding environment, the corneal epithelium is the layer most susceptible to damage. While a superficial corneal abrasion may fully heal within days, severe injuries can take several weeks to heal, while some never fully recover. Even when the wound is completely healed, a condition called RCE may develop, wherein the corneal epithelial cells will sporadically shed resulting in extreme pain and discomfort. RCE is found to be 1 in 150 [9] individuals and additionally patients with lattice/granular/macular dystrophy have shown an increased risk of obtaining RCE [9]. Although the true biological cause of RCE is unknown, it is speculated that the sporadic peeling i1.3.1s due to poor corneal epithelial cell attachment to the underlying Bowman's membrane [10]. Furthermore, this can be supported by an overabundance of matrix metallopeptidase (MMP) enzyme upon corneal injury {Sobrin, 2000 #16}.

RCE may include symptoms such as severe eye pain, lacrimation, and corneal scarring leading to visual changes. Typically, if the eye lacks the sufficient lubrication (i.e. during sleep), any movement of the eye may also trigger denuding of the epithelium. This sporadic nature may therefore cause further psychological complications such as photophobia and insomnia [2].

1.3.1 Matrix Metalloproteinase Enzymes

It has been shown that when afflicted with RCE, multiple biological factors and enzymes are secreted in order to reduce inflammation, increase wound healing speed and remove any debris or injured cells. Several MMPs are upregulated during RCE including MMP-2, MMP-8 and MMP-9 [11]. These MMP enzymes are responsible for degradation of the extracellular matrix [10],

which involves the dissolution of the Bowman's layer to allow for regrowth and healthier cell-membrane adhesion. MMP-8 has demonstrated a higher number of cleavage sites (n=352) to that of MMP-9 (n=161) and was additionally shown to degrade gelatin at a faster rate {Eckhard, 2016 #78}{Marion, 2006 #320}.

Studies have indicated that an overabundance of MMP-9 is the cause of RCE [13-15], however, no specific concentration is given. It is shown that corneal-related diseases cause MMP-9 levels to fluctuate in the low hundreds of ng/mL [16, 17].

1.3.2 Current Commercial Solutions

Once diagnosed with RCE, ophthalmologists follow a flowchart of treatment methods as shown in Figure 2. The flowchart is organized so that the least invasive therapies are implemented prior to the more aggressive surgeries.

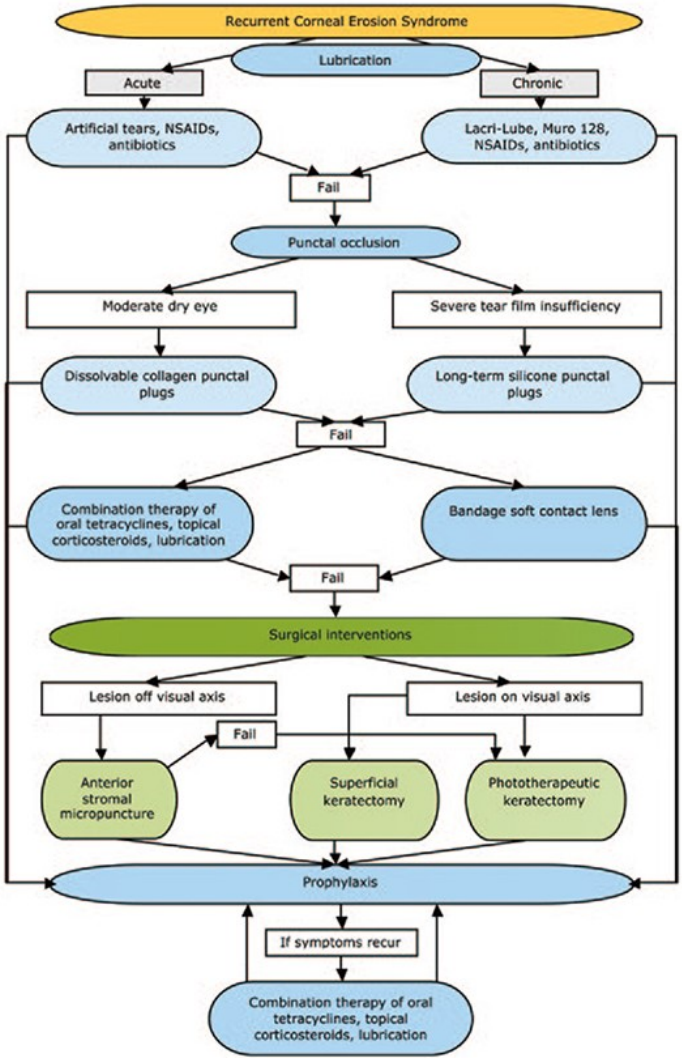

Figure 2. Treatment options for RCE [2]

A simple lubrication using eyedrops is initially attempted over the course of the first week. The eye drops may contain either an anti-inflammatory or a wound-accelerating drug to aid in the healing [2].

If ineffective, punctal occlusion can be used as an indirect form of lubrication. Once inserted into the tear duct, the tear film experiences a reduced drainage rate due to the blocked passageway which allows for a higher tear retention. Insertion of a punctal occlusion is a painless technique that can be performed in a matter of minutes and can be removed quickly should any side effects arise [2].

Regular contact lenses should be avoided during this phase due to potential scraping of the damaged area, and possible loss of oxygen to the eye, however, a bandage contact lens (BCL) can be used instead. This special type of lens is a medical-graded contact lens that RCE patients wear to protect the nerve endings and reduce pain. The lens also possesses an increased oxygen permeability allowing it to be used continuously for a week long period (day and night) [2].

If all previous treatments fail, ophthalmologists may attempt an invasive surgery. Operations are generally avoided due to surgical complications that may arise. Most surgery options for RCE involve superficial damage to the Bowman's membrane in an attempt to re-trigger the healing process and secure a strong cell-membrane adhesion.

1.3.3 Current Issues

During the day, lubrication of the eye is normally not an issue as the surface is constantly replenished with new tears. Although the lacrimal turnover rate in the eye is slow ($0.6 - 1.4\mu L/min$) [18], any excess instilled fluid may be removed in a matter of minutes, thereby removing compounds that may further cause irritation. This poses a problem when the cornea is in need of external aid such as eye drops. Most drug solutions are removed in a matter of minutes, resulting in only 5% of the active ingredient being absorbed into the eye [19]. This forces the consumer to follow an unpleasant and strict regime of applying the eye drops 6-8 times every day.

Punctal occlusions may cause excess obstruction to the tear drainage, resulting in epiphora or unwanted tearing. The occlusion may become lodged in the tear duct causing swelling and pain as well as infection. The wedged occlusion can be removed using forceps [2], however, another regime of antibiotic eye drops must be implemented to minimize infection. As punctal occlusion only helps to avoid future erosions through reduction of friction, the cornea is vulnerable to denuding through other means.

BCLs are a common method to act as a barrier to the external environment. Although effective in improving patient comfort, they still require antibiotic eye drops at least twice a day. These eye drops do not provide any sort of active ingredient that aids in restoring the corneal epithelial cells, and as such, the restorative process may take between 2-8 weeks.[2]

Surgery is often avoided due to the invasiveness and will only be considered after thorough medical therapies have been attempted. Aversion to surgical procedures are normal as they may cause scarring, inflammatory responses and infections, among other complications [2].

Although other forms of commercial treatments exist [20], the ones stated in this report are the most commonly implemented therapies [2]. These commercial remedy options either lack an appropriate active ingredient that improves corneal wound healing and cell adhesion to the underlying membrane, or they are inefficient due to their low bioavailability.

1.3.4 Current Research Solutions

Current research fails to specifically address RCE as there exists an emphasis on techniques to improve the delivery of various compounds to both the surface *and* interior of the eye. These studies focus on either the material delivering the drug or on conjugating/encapsulating the drug itself for longer retention in the tear film. Specific research areas may include the incorporation of nanoparticles in contact lens materials, inclusion of diffusion barriers, molecular imprinting or plasma treatment as will be briefly discussed in this section.

Nano- and micro- carriers have been extensively studied as a mechanism to encapsulate drugs {ElShaer, 2016 #323}{Prakash, 2017 #324}. Encasing a drug holds several advantages such as increasing the half-life and retention time as well as providing a targeted delivery to a specific area or section of the eye. These micro-particles are polymer materials that can be optimized for either targeted delivery or to help the carrier pass through certain hydrophobic portions of the tear film. Conjugations directly on the drug are not viable as an alteration may affect its bioactivity or half-life [21]. Although efficient for targeted drug delivery, the fabrication procedures to create nano-/micro-carriers are complex and their respective shelf-lives in existing eye drop solutions have not been thoroughly investigated [23]. Furthermore the toxicity of implementing nano-/micro-carriers is not well studied {Bahadar, 2016 #23}.

Diffusion barriers have been utilized to force the active ingredient to diffuse through an extended convoluted path to reduce the release rate. Vitamin E loading into an existing NIGHT&DAY^{TM}

lens has demonstrated to increase both loading and release time of timolol, however, at a cost of slightly reducing the oxygen permeability and significantly decreasing the ion permeability {Peng, 2010 #314}.

Materials have been created in order to improve and retain a longer release profile of specific molecules. Molecular imprinting is an example of a technique used during the fabrication process of a material in which a cavity in the shape of the desired drug to be delivered is created [24]. By doing so, both an increase in the amount of drug loaded into the polymer matrix and a decrease in the burst release of the drug into the surrounding environment results. This technique has shown promise for delivering a single drug, however, it is not a scalable option for other applications and it requires an intricate fabrication procedure that is not easily implemented in existing commercial products [24].

Modifying existing commercial products to be viable as drug carriers is an ongoing research field concerning eye related diseases. For example, plasma treatment can be used to both increase the wettability and decrease the initial drug release kinetics thereby having a lower burst release [25]. The surface modifications that plasma treatment offer are not permanent and an average consumer would not have access to a plasma treatment machine to readjust their lens. Alternatively, incorporating the drug directly into the polymer solution prior to crosslinking of the contact lens has been investigated to increase the amount of drug loaded [26]. This is a viable solution for molecules with a high half-life, but it still does not address the low bioavailability of drug delivered to the eye as a rapid release of drug will still exist.

The solutions being investigated in research all possess their own advantages and although each method is practical, they are not very scalable, are difficult to implement in existing commercial products or require complex fabrication procedure.

1.4 Molecules to Aid in Corneal Epithelial Wound Healing

A variety of molecules have demonstrated the ability to accelerate wound closure [27]. An extensive literature review on the list of molecules available to accelerate corneal epithelial wound healing was performed including investigations on growth factors, extracellular matrix components, and molecules of high and low molecular weights. The potential active agents to be

examined was reduced after disregarding molecules with a short half-life (less than one week), were too expensive to implement in a controlled release system, or required conjugation to deliver (i.e. small molecules <~40kDa in size). As such, two molecules were selected for this project: bovine lactoferrin (BLf) and hyaluronic acid (HA).

1.4.1 Bovine Lactoferrin

BLf is a ~80kDa globular glycoprotein commonly found in secretory fluids that operates in the body's immune system by providing antibacterial functions [28]. The lactoferrin molecule may be secreted and purified from human milk and cow milk, with bovine milk estimating a concentration of 150mg/mL [29]. BLf is an approved additive for infant growth supplements in several countries and is currently under revision by the US Food and Drug Administration (FDA) for being "generally recognized as safe" (GRAS) [30].

Lactoferrin is comprised of a C- and N-lobe. The N-lobe is well studied and praised for its bacteriostatic effect [31], however, the C-lobe of BLf instigates various medical therapeutics including wound healing in immortalized limbal epithelial cells, boasting an increase of nearly 200% at the 24-hour mark in an alkali wound model [32]. Despite the C-lobe being the active group in corneal wound healing, it has been shown that the bovine glycoprotein as a whole is capable of accelerating corneal epithelial wound healing *in vitro* [32, 33].

1.4.2 Hyaluronic Acid

HA is the only exclusively non-sulfated glycosaminoglycan (GAG) composed of linear polysaccharides (Figure 3) that is found in large amounts in humans (15g in an average 70.kg person [34]). HA is responsible for numerous functions in the human body including a critical role in the extracellular matrix for cell migration and proliferation [35]. As a polysaccharide, the molecular weight of this compound may range between <5kDa to in the millions.

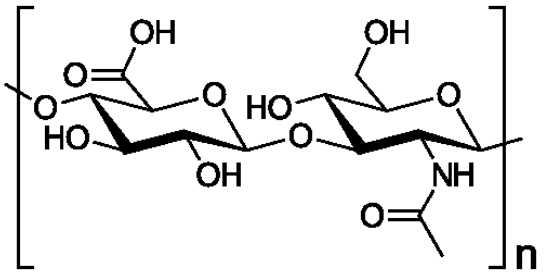

Figure 3. Molecular structure of HA

HA has demonstrated the ability to improve rabbit corneal epithelial wound healing *in vivo* in *n*-heptanol, iodine vapour and mechanical scraping models [36]. Although different lengths of HA exist, no significant evidence suggests that a particular molecular weight is advantageous over another in corneal wound healing [37] as both the native molecular weight as well as oligomer length HA (5-10kDa) have demonstrated accelerated wound healing [38, 39].

1.5 Ideal Controlled Release

Upon entering the bloodstream, the majority of drug is immediately cleared by the kidneys and liver causing the therapeutic effect to be brief [40]. For example, when a pill is ingested, a fraction of the drug will be taken up by the intestines, and less will pass through the renal clearance. To avoid the intestinal barrier, doctors can opt to directly incorporate the drug (if viable) into the body intravenously. This way, the initial renal clearance will be bypassed and 100% of the drug will be incorporated into the plasma, however, the first cycle through the kidneys will cause a loss of the majority of drug in the blood.

In order for medication to be effective, the concentration of active ingredient must be within a therapeutic window. If below the lower limit, the drug will not cause an effect; whereas above a threshold may result in toxic side effects [41]. The presence and clearance of a drug can be illustrated in a pharmacokinetic curve (Figure 4). This diagram is also representative of eye drops applied to the surface of the eye. As most of the drug is immediately cleared by the tear film, the remaining concentration will be absorbed (increase in curve) and promptly filtered (decrease) from the system.

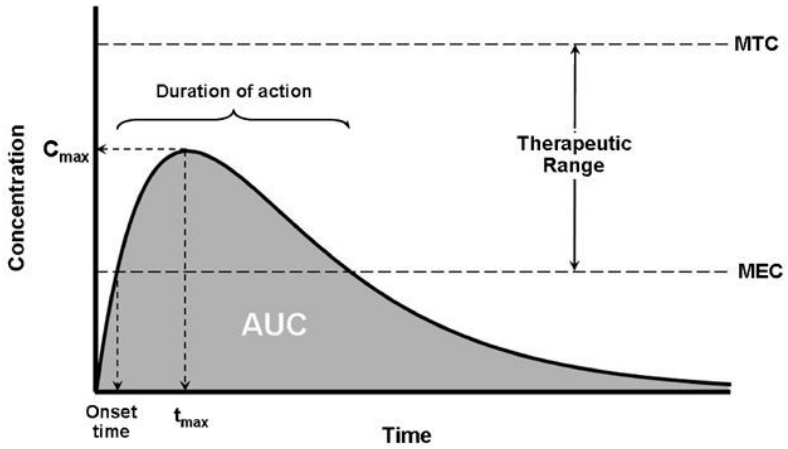

Figure 4. Typical pharmacokinetic curve [41]. AUC= area under curve, MEC = minimum effective concentration, MTC = minimum toxic concentration

Ideally, a controlled drug delivery system is able to sustain a constant release of active ingredient to maintain a drug concentration level within the therapeutic window for a specified period of time.

1.6 Gelatin Methacrylate

As the ocular drug delivery system is in contact with the cornea, the selected material must be transparent and able to conform to the shape of the eye without causing irritation. Gelatin methacrylate (GelMA) was chosen for this project due to its odorless, transparent properties, biocompatibility and tunable properties {Matthyssen, 2018 #316}{Wang, 2017 #317}. GelMA is derived from the FDA approved gelatin, which is a denatured form of collagen.

Food grade gelatin is broken down from a mixture of by-products from meat and leather industries such as cattle bones and pig skin [42]; therefore its molecular weight and structure varies depending on the source and method of denaturation. It has been determined that the general breakdown of gelatin includes mixture of peptides and proteins containing proline, hydroxyproline and glycine in its polypeptide chain [43].

GelMA is a modified form of gelatin that is complexed with methacrylate anhydride (MA). The product, after lyophilisation, can be solubilized in a photoinitiator (PI) solution and eventually crosslinked (Figure 5). GelMA can be tuned by varying the amount of MA added during the reaction. A higher methacrylation degree will translate to higher crosslinking and therefore a

stronger gel. Furthermore, the concentration of GelMA powder in PI solution can be altered to fabricate a dense or light gel.

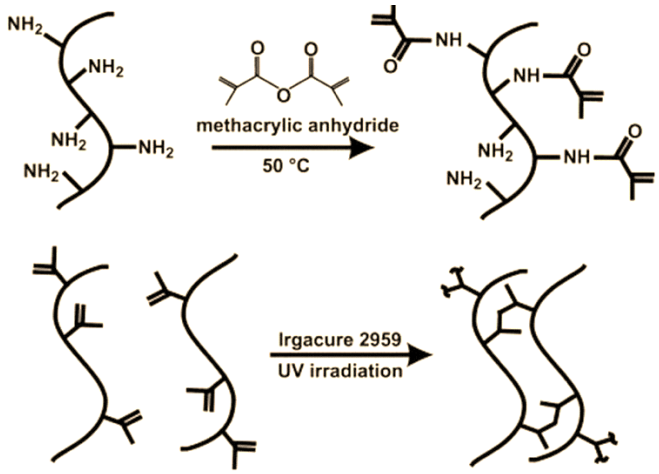

Figure 5. Reaction mechanism of GelMA fabrication [44]

As a derivative of gelatin, GelMA is also degraded by the collagenase enzymes, specifically MMP-9 [45]. This enables GelMA as a viable material for controlled release delivery due to its tunable properties through adjustment of methacrylation degree, concentration of polymer and UV dosage {Zhao, 2016 #325}. GelMA can additionally act as a mechanism to consume the collagenase.

1.7 Objective and Research Question

The objective of this thesis was to deliver an active ingredient such as BLf or HA using an enzyme-controlled GelMA hydrogel. Tuning properties such as the methacrylation degree of the GelMA and concentration of GelMA in PI solution will allow for a sustained and steady release of molecule. The research questions that are being investigated in this project are:

1. Gelatin methacrylate is a tunable hydrogel that is able to release a mid-range molecule (50-100kDa) over a targeted seven days
2. Incorporation of BLf or HA *in vitro* will significantly improve human corneal epithelial (HCEpC) in a scratch wound and PDMS wound assay model

The research questions can be further broken into aims:

1. Validation of a model molecule of ~70kDa size and influences of other solute and gel components that can vary the results.
2. Determination of the controlled release profile under various methacrylation degree, concentration of GelMA and UV dosage.
3. Determination of an appropriate wound assay model and selection of molecule to accelerate wound healing.
4. Validation and examination of bioactivity and controlled release profile of selected molecule on a wound assay.

2.0 Materials and Methods

The materials and methods sections are organized into three primary sections: controlled release experiments (section 2.1.1 and section 2.3), wound assay studies (section 2.1.2 and section 2.4), and optimization of design (section 2.1.3 and section 2.5), respectively.

2.1 Materials

2.1.1 Controlled Release Studies

The GelMA used for the controlled release and drug loading studies were made from type A gelatin. Type A gelatin, IRGACURE 2959 and MA were obtained from Sigma. Phosphate-buffered saline (PBS) that was used as the reaction medium was purchased from Fisher Scientific. The centrifuge used to remove impurities was a Sorvall ST 16R centrifuge purchased from Thermo Scientific. Dialysis was performed using 12,000-14,000Da molecular weight cut-off tubing (Spectra/Por®). A FreeZone 1L freeze-dryer from LABCONCO used to lyophilize the GelMA solution. Both collagenase type IV/MMP-9 and MMP-8 were purchased from GIBCO, ThermoFisher. Crosslinking of GelMA solutions was performed with either an HTBX UVLED curing oven from EIGHT-LED (365nm wavelength with 600mW/cm^2 at 100% power) or the FB-UVXL-1000 UV-crosslinker (265nm wavelength with 120mJ/cm^2) from Fisher Scientific. The 70kDa and 4kDa Fluorescein isothiocyanate (FITC)-dextran were purchased from Sigma.

2.1.2 Wound Assay

2.1.2.1 Rabbit corneal epithelial Cell Culture

Primary rabbit corneal epithelial cells (RCEpCs) along with its respective epithelium cell media (EpCM) kit (including insulin-transferrin-selenium, epidermal growth factor, L-glutamine, antibiotic-antimycotic solution and fetal bovine serum (FBS) supplements) and gelatin-based coating solution were purchased from Cell Biologics, Inc. The cells were passaged using trypsin-EDTA from GIBCO Thermo Scientific. The FBS and dimethyl sulfoxide (DMSO) that were used to freeze the cells were acquired from GIBCO Thermo Scientific and Sigma, respectively.

2.1.2.2 Human Corneal Epithelial Cell Culture

HPV-immortalized HCEpCs were generously provided by Dr. Maud Gorbet, PhD, University of Waterloo, ON. Keratinocyte serum free media supplemented with keratinocyte growth serum (KGS) and penicillin/streptomycin (P/S) was utilized as the primary growth medium (fully supplemented media will be abbreviated as KM) and purchased from Sciencell. The HCEpCs were passaged with TrypLE reagent obtained from GIBCO by Life Technologies from Thermo Scientific.

2.1.2.3 Bioactivity Assay and ELISA

Both 500kDa and 60kDa HA were purchased from Lifecore™. The enzyme linked immunosorbent assay (ELISA) kit was acquired from Echelon Biosciences.

2.1.3 Optimization

Biofinity contact lenses (CLs) from CooperVision possessing a back curvature of 8.6mm, 14.0mm diameter and -3.00 power were generously donated from Dr. Lyndon Jones, PhD, Centre for Ocular Research & Education, University of Waterloo, ON. Sonication was performed using a Durasonix DR-MH 100 ultrasonic cleaner. Polyvinyl alcohol (PVA) was acquired from Sigma. Polyethylene terephthalate (PET) sheets were purchased from Goodfellow. The mechanical strength was tested using a CETR UMT-2 tribometer.

2.2 Methods

2.3 Controlled Release

2.3.1 GelMA Preparation

Type A gelatin was mixed in PBS using a glass bottle to make a 10% (w/v) solution at 50°C for one hour or until fully dissolved. MA was then added to the gelatin solution at a ~0.5mL/min rate to ensure homogeneity. The amount of MA added varied depending on the desired methacrylation degree. Once added, the mixture was stirred to react for one hour at 50-60°C. The reaction was stopped by adding a 1X dilution of ~40°C PBS. Impurities and low molecular weight GelMA were removed through a centrifugation step of 5000RPM for 5 minutes. The supernatant was collected and placed in a 12-14kDa dialysis tube for dialysis in deionized (DI) water. The DI water was changed every 2 hours in an 8-hour period for the first two days and daily thereafter for 5-7 days. The DI water was kept at ~40°C during the entirety of this process to prevent the GelMA from physically gelling. The GelMA solution was then placed in 50mL centrifuge tubes and freeze-dried at -80°C for a week to remove the water content, leaving a white crystalline powder. The lyophilized powder was stored at -20°C or -80°C.

2.3.2 GelMA Patch of FITC-dextran Gel Fabrication

IRGACURE 2959 PI was dissolved in PBS at 60°C for one hour to make a 0.5% solution. The lyophilized GelMA made in section 2.3.1 was dissolved in the 0.5% PI solution in a screw-top cryogenic tube (to minimize evaporation) at 60 °C for two days to ensure the powder was completely solubilized. FITC-dextran of either 4kDa or 70kDa molecular weight was added to the solution to achieve a 5mg/mL concentration. This mixture was vortexed for 10 seconds to ensure homogeneity. To remove any bubbles formed from agitation, a 5000RPM centrifugation step was performed for five minutes. The solution was then heated to 60°C in an oven to reverse any physical gelling that may have occurred during the centrifugation step. Approximately 200μL of the GelMA-FITC-dextran solution was pipetted into a transparent holding chamber composed of glass slides of dimensions 22mm x ~15mm x 0.5mm (Figure 6). An optional one hour refrigeration step (to induce physical crosslinking) was implemented prior to placement in the HTBX UVLED curing oven at various intensities for 300s. The compartments were disassembled and the solid gel was cut into 6mm diameter cylinders.

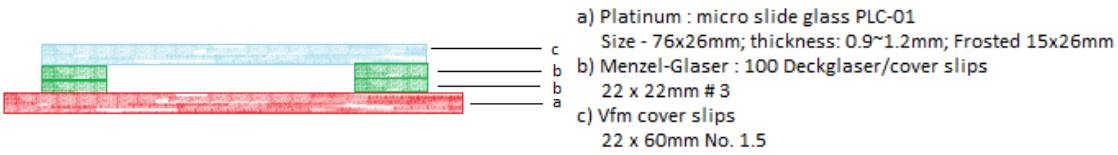

Figure 6. Schematic of chamber for GelMA fabrication

2.3.3 Controlled Release of FITC-dextran through Enzymatic Degradation of GelMA

The GelMA disks created in section 2.3.2 were placed in a 24-well plate and incubated at $37°C$. PBS was added to the well for 30 minutes as a wash step to remove any surface adsorbed molecules. The PBS was then removed and 1mL of PBS, 250ng/mL, $1\mu g$/mL, or $50\mu g$/mL MMP-9 in PBS was added to each well. The liquid was replaced at 2, 4, 6, 8, 10, 12-hour mark and every 24 hours for 7 days. The removed liquid was placed in a 48-well plate and stored in -80°C until ready to be quantified. At the end of the experiment period, $200\mu g$/mL MMP-9 in PBS was added overnight to completely degrade the GelMA disk. The solution was then stored in a 48-well plate until ready to be quantified.

$100\mu L$ of FITC-dextran liquid at each time point was transferred to a black 96-well plate and its fluorescence was quantified using a Biotek Synergy 4 plate reader. The samples were characterized at a fluorescence excitation at 490nm and emission of 520nm. The accumulative release was calculated in Excel using a FITC-dextran calibration curve and graphed using GraphPad Prism.

2.4 Wound Assay Studies

2.4.1 HCEpCs Wound Assay

HCEpCs were cultured in a T-25 flask using KM media that was changed every other day. At ~90% confluency, they were passaged in 2mL of TrypLE for 10-15 minutes and sub-cultured in a bare 24-well plate (for the scratch wound assay) or a 24-well plate containing a thin, punched out PDMS stamp adhered to the surface. The cells were then supplied with KM until a monolayer was formed. For a scratch wound assay, a P200 pipette tip was scratched in a "+" shape (Figure 7a); for the PDMS wound assay, the PDMS was carefully stripped from the surface (Figure 7b). The well was then rinsed with PBS and replaced with KM media containing HA or BLf of appropriate concentration. The media was changed with fresh KM media daily or with KM containing the

respective drug and concentration of each well. Images were taken daily to observe the closure of the wound and graphs were generated using GraphPad Prism.

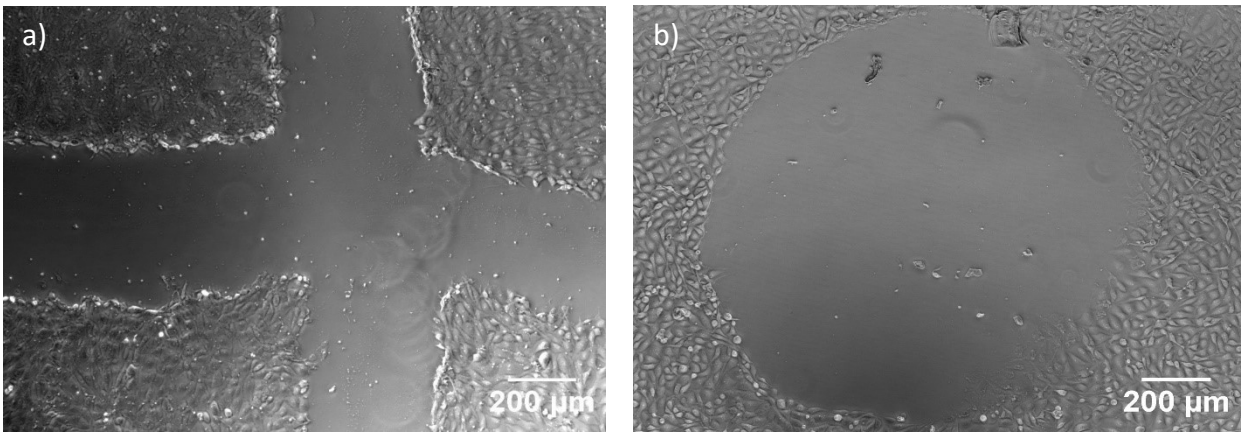

Figure 7. Scratch and PDMS wound assay initial wounds

2.4.2 RCEpCs Scratch Wound Assay

RCEpCs were cultured using a T-25 flask in EpCM. Once the cells attain ~90% confluency, they were briefly rinsed with PBS and passaged in 2mL of trypsin-EDTA for 3-5 minutes. The trypsin-EDTA was then aspirated and 8mL of EpCM supplemented with 10% FBS was added. The cells were then sub-cultured on a 24-well plate surface pre-coated with a gelatin-based coating. The media was changed daily until a cell monolayer was formed. Either a scratch wound assay or PDMS wound assay was performed identical to that described in section 2.4.1. The well was then rinsed with PBS and replaced with EpCM containing either HA or BLf of appropriate concentration. Media was changed daily with fresh EpCM until full closure of wound. Images were taken daily to observe the closure of the wound and graphs were generated using GraphPad Prism.

2.4.3 Bioactivity Assay

GelMA patches were created as described in section 2.3.2 containing various concentrations of 60kDa HA. Upon crosslinking the GelMA under 600mW/cm^2 for 300s, 8mm patches were created and placed in a 24-well plate. KM media containing KGF and P/S was added to the well and replaced at the 12, 36, 60-hour and every 24 hours afterwards for 5 days. The replaced media was stored in a separate 24-well plate in -80°C until a wound assay was prepared. HCEpCs were prepared and a wound assay was created as described in 2.4.1. After the washing step, the PBS was removed either KM or the collected 12 hour time point was added. The media was then

replaced every 24 hours with the continuing stored time points until the wound was healed. Images were taken every 12-24 hours to monitor the rate of wound healing and curves were created using GraphPad Prism.

2.4.4 ELISA Determination of Hyaluronic Acid

An HA ELISA was performed as per the Echelon, Inc assay procedure. Either samples, standards, or diluent was added to the wells in appropriate amounts and $50\mu L$ of working detector was added to each well except the black control wells. The plate was then covered with a plate seal and incubated for one hour at $37°C$. $100\mu L$ of each sample was then transferred to the detection plate provided and gently mixed. The detection plate was covered and incubated at $4°C$ for 30 minutes. The solution was then removed from the plate and washed with 1X wash buffer. Once sufficiently rinsed, $100\mu L$ of working enzyme was added to each well and incubated at $37°C$ for 30 minutes while covered with a plate seal. The solution was removed and each well was rinsed with wash buffer. $100\mu L$ of working substrate solution was then added to each well and the plate was incubated at room temperature in a dark environment. The absorbance at 405nm was measured at 15 minutes and 30 minutes and the reaction was stopped by adding $50\mu L$ of stop solution to each well. A best fit curve was generated using non-linear regression analysis with GraphPad Prism and a sigmoidal dose response-variable slop curve (four-parameter) analysis was used to determine the concentration of each well as described in the Echelon procedure.

2.5 Optimization

Each CL was prepared by initially rinsing with DI water and subsequently drying overnight at $60°C$ to remove excess liquid. The lenses were then cut into 4mm diameter circles and used for experimentation.

2.5.1 Patterning of GelMA patch

GelMA disks were prepared similar to that mentioned in section 2.3.2. $200\mu L$ of the solution was pipetted into a transparent holding chamber composed of patterned PET of dimensions 22mm x ~15mm x 0.5mm. In order to maintain shape and solidify the solution prior to crosslinking, the chambers were placed at $-4°C$ for one hour prior to a 6mW/cm^2 300s exposure to UV. The compartments were disassembled and the solid gel was cut into 6mm diameter cylinders. The samples were then degraded in a similar fashion as mentioned in section 2.3.3.

2.5.2 Transmission, Wettability, Mechanical Strength Characterization

CLs were soaked overnight in 10% or 30% GelMA solution in PBS in a fastened micro-centrifuge tube at $37°C$. The lenses were removed from the sample and the exterior was wiped with Kimwipe to remove any excess reagent. The samples were then placed in a FB-UVXL-1000 UV-crosslinker (265nm wavelength at 120mJ/cm^2). The CLs were then either characterized for light transmittance, surface wettability using DI water and mechanical strength up to 50% strain.

2.5.3 Drug Loading through Sonication

CLs were soaked in either a GelMA solution containing 70kDA FITC-dextran at $60°C$ overnight (control), sonicated for 30 seconds in DI water and then placed in GelMA containing 70kDa FITC-dextran and left to incubate overnight in $60°C$ (SONDION), or sonicated for 30 seconds the morning after an overnight incubation in GelMA containing 70kDa FITC-dextran (ONSON). Each sample was placed in securely fastened micro-centrifuge tube (to avoid evaporation). The samples were then removed from their respective incubation mediums and gently patted down with Kimwipes to remove excess GelMA. The lenses were UV irradiated for 300s at 600mW/cm^2 and placed in 24-well plates containing $100\mu g$/mL of MMP-9 to degrade the GelMA overnight. The amount of FITC-dextran loaded was calculated by comparing the solution containing degraded GelMA to a 70kDa FITC-dextran calibration curve.

2.5.4 Drug Loading through Freeze-Drying

CLs were stored in a 15mL centrifuge tube in -20$°C$ until ready to freeze-dry. The tube was then placed into a freeze-drying flask and attached to the freeze-drier overnight. After removing the samples from the tubes, the lenses were incubated in GelMA containing 70kDa FITC-dextran overnight at $60°C$. Upon 300s UV irradiation at 600mW/cm^2, the samples were wiped with Kimwipes and degraded overnight in a well plate using $100\mu g/mL$ MMP-9 in PBS. The amount of FITC-dextran loaded was calculated by comparing the solution containing degraded GelMA to a 70kDa FITC-dextran calibration curve.

2.5.5 Extra Dipping

CLs were soaked overnight in GelMA containing 70kDa FITC-dextran at $60°C$. After a brief patting down using Kimwipes, the samples were then placed under UV for 300s. The lenses were then dipped into the GelMA solution once more and UV irradiated a second time. Once completed, the samples were degraded in a 24-well plate containing $100\mu g/mL$ MMP-9 in PBS. The amount of FITC-dextran loaded was calculated by comparing the solution containing degraded GelMA to a 70kDa FITC-dextran calibration curve.

2.5.6 Alternate Interior Medium

CLs were incubated overnight in GelMA containing 70kDa FITC-dextran in a 5% PVA solution of PBS at $60°C$. The CLs were removed the following morning and UV irradiated for 300s at 600mW/cm^2. The samples were then degraded in a 24-well plate containing $100\mu g/mL$ MMP-9 in PBS. The amount of FITC-dextran loaded was calculated by comparing the solution containing degraded GelMA to a 70kDa FITC-dextran calibration curve.

2.6 Statistics

Statistics were calculated using Graphpad Prism 6 using one-way analysis of variance (ANOVA) (and non-parametric) analysis for single comparisons and two-way ANOVA for multiple comparisons (such as the wound assays). T-tests were calculated using Graphpad Prism for the bar graphs.

3. Results and Discussion

3.0 FITC-dextran Calibration Curve

This section focused on the validity of 70kDa FITC-dextran as a model molecule for the controlled release studies and investigated the factors influencing its fluorescence in a calibration curve to obtain an accurate reference to quantify the controlled release studies. These factors included: UV-irradiation, elevated temperatures, reagents used in the controlled release experiments, and impurities present during GelMA fabrication.

3.0.1 Effect of UV and Incubation on Fluorescence Intensity

Two primary external influences that affected the stability of FITC-dextran were the UV irradiation and the 5-7 day incubation in a $37°C$ + 5% CO_2 environment. An investigation on the

degree of influence UV irradiation had on FITC-dextran was performed on the calibration curve (Figure 8a). The UV exposure was examined using an FB-UVXL-1000 UV-crosslinker (265nm, 120mJ/cm^2) and an HTBX UVLED curing oven (365nm wavelength with 600mW/cm2 at 100% power). It was noted that the HTBX UVLED machine at >= 300mW/cm^2 caused significant quenching of the FITC-dextran as the colour of the precursor GelMA solution transformed from a bright yellow solution to a colorless, crosslinked hydrogel.

A similar experiment was performed with a FITC-dextran calibration curve that was subjected to 10 days in a 37°C+5% CO_2 incubator compared to one that was freshly created (Figure 8b).

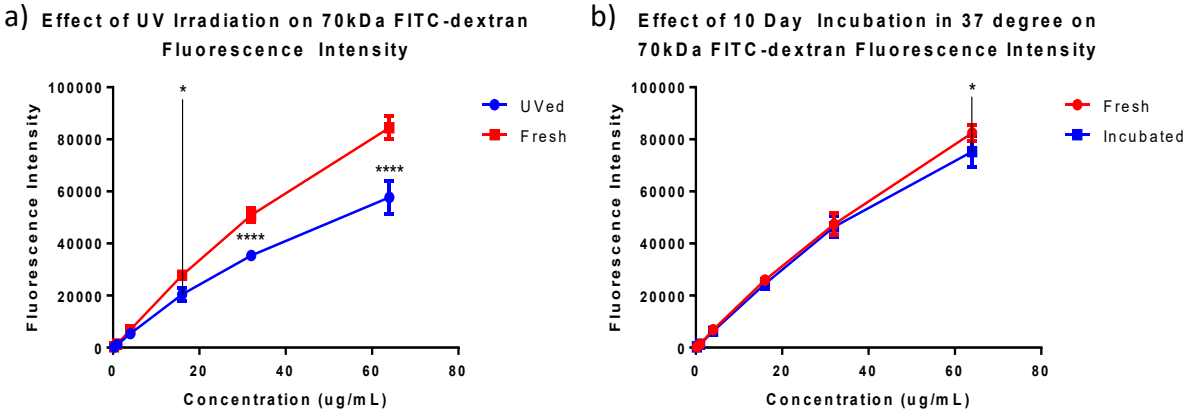

Figure 8. Effect of a) UV; *: p <0.05, ****: p<0.0001 or b) 37°C incubation; *: p<0.05 on FITC-dextran fluorescence intensities at 250ng/mL, 1$\mu g/mL$, 4 $\mu g/mL$, 16$\mu g/mL$, 32$\mu g/mL$ and 64$\mu g/mL$ concentrations (n=3). Error bars shown are SD.

Exposure to UV light significantly quenched the calibration curve. The lowest concentration (250ng/mL) of FITC-dextran demonstrated a 25% discrepancy between the fresh calibration curve and the UV irradiated sample. This effect became stronger at 64$\mu g/mL$ with a 32% quenching. The decrease in fluorescence intensity can be explained by two mechanisms: static and dynamic quenching [46].

Static quenching involves creating a non-fluorescent complex before excitation (i.e. before UV crosslinking) of the fluorophore which causes a decrease in fluorescent intensity [47]. Dynamic (or collisional) occurs when an excited fluorophore comes into contact with an atom or molecule that can facilitate non-radiative transitions (with a quencher) back to the ground state [47].

As UV irradiation excited the fluorophore molecules (FITC), energy will be released in the form of radiation or heat. This energy can be transferred to other molecules, in which case they may absorb excess energy causing the original fluorophore to lose fluorescence. It has also been shown that at higher concentrations of fluorophore, collisional quenching may occur between the molecules themselves [48]. Furthermore, Shauenstein et al. [49] has demonstrated that a high concentration of FITC causes a shift in emission spectra, which may further decrease fluorescence upon UV irradiation. These two phenomena would explain the higher discrepancy at the $64\mu g/mL$ concentration of FITC-dextran and why it became more sensitive to the 365nm UV exposure than once anticipated. In general, as literature cites an optimal wavelength for crosslinking GelMA of 365nm [45, 50], the HTBX UVLED machine was used.

The elevated temperature of $37\,°C$ did not cause any significant decrease in intensity until concentrations of higher than $30\mu g/mL$ FITC-dextran. As no time point in the controlled released experiments contained a concentration greater than $30\,\mu g/mL$ (shown in section 3.1), the $64\mu g/mL$ concentration in the calibration curve may be removed and a parallel incubation in $37°C$ is not necessary. Although the increased temperatures did not show a significant difference until a concentration of $64\mu g/mL$ FITC-dextran, temperature has previously been shown to influence quenching of fluorophores [51]. Fraiji et al. [46] experimented on the time-dependent nature of fluorescence and noted an increased temperature caused an accelerated dynamic (collisional) quenching and a slower static quenching. It is speculated that the decreased fluorescence reading at concentrations greater than or equal to $64\mu g/mL$ FITC-dextran is the result of a synergistic effect between the concentration-dependent collisional quenching and the accelerated dynamic quenching due to elevated temperatures.

3.0.2 Effect of Reagents on Fluorescence Intensity

The effect of each reagent on the quantification of the calibration curve was investigated. These calibration curves were compared to a control containing identical concentrations of 70kDa FITC-dextran in PBS (Figure 9). All samples (aside from the control) were degraded overnight using $100\mu g/mL$ MMP-9 in PBS. Gelatin type A (GelA) was used instead of GelMA to compare the PBS and IRGACURE PI in PBS solutions to avoid the influence of crosslinking on the results.

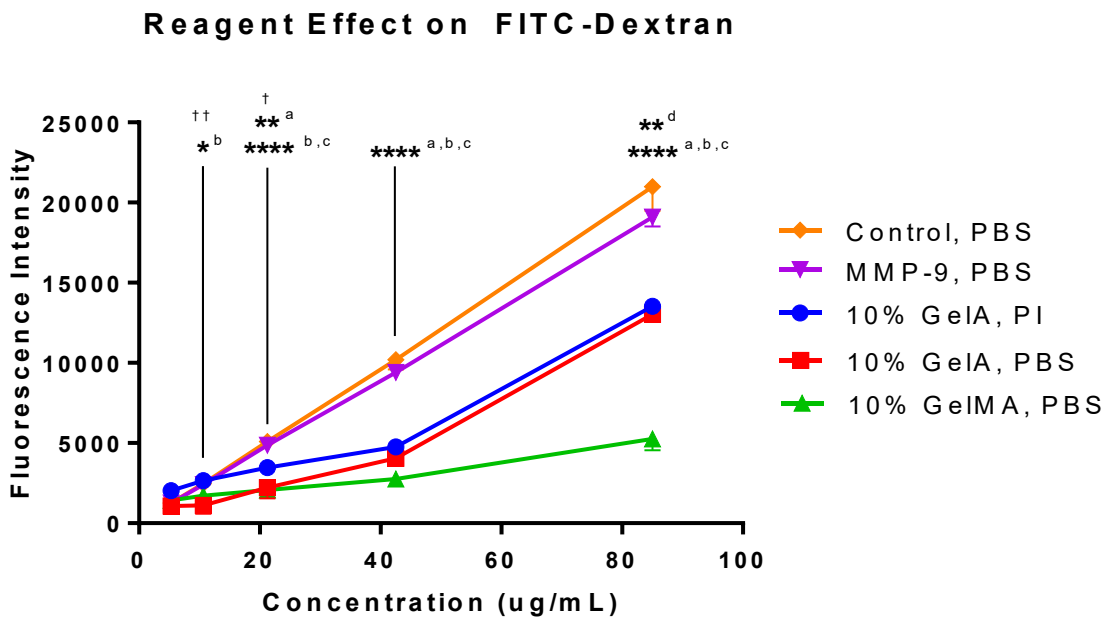

*Figure 9. Effect of Reagents on FITC-dextran reading compared to control sample (70kDa FITC-dextran in PBS with no additives) (n=2). Error bars shown are SD. Statistical significance represents comparison between control and a – 10% GelA, PI; b - 10% GelA, PBS; c – 10% GelMA, PBS; d – MMP-9, PBS. *: p<0.05, **: p<0.005; ****: p<0.0001. † represents a comparison between 10% GelA, PI vs 10% GelA, PBS samples. †: p<0.05; ††: p<0.01*

Most reagent (GelMA, GelA and MMP-9) demonstrated a negative influence on the fluorescence signal. Although the concentration of reagent (GelA, GelMA and MMP-9) utilized in these experiments was larger than that in the controlled release experiments, the presence of these substances could synergistically decrease the intensity of the calibration curve.

The presence of $100\mu g/mL$ MMP-9 in PBS (purple curve) significantly inhibited the intensity readings compared to the control as the concentration of FITC-dextran increased as shown in the ~$85\mu g/mL$ points ($p < 0.01$). This could be due to a mechanism wherein the MMP-9 caused the FITC to be more sensitive to dynamic quenching at higher concentrations.

The addition of GelMA (green curve) diminished the fluorescence intensity severely compared to the control. It was discovered that the addition of GelMA also reduced fluorescence compared to a similar solution containing GelA (red curve). This discrepancy could be due to the presence of the MA functional groups or any residual impurities still present from the fabrication procedure (as demonstrated in section 3.0.3).

It is unclear if the GelA or GelMA are screening (blocking of fluorescence) the fluorophore or if complexation is occurring between FITC-dextran and the amino groups on GelA (which would also be present on GelMA) (Figure 10) [52]. This would result in a decrease in the recorded emission intensities as demonstrated by Shauenstein et al. [49]. As FITC-dextran is stable at high temperatures [53], and the isothiocyanate functional group is complexed with the –OH group on the dextran polysaccharide, it is unlikely that this conjugation of FITC would favourably react with the free amine groups.

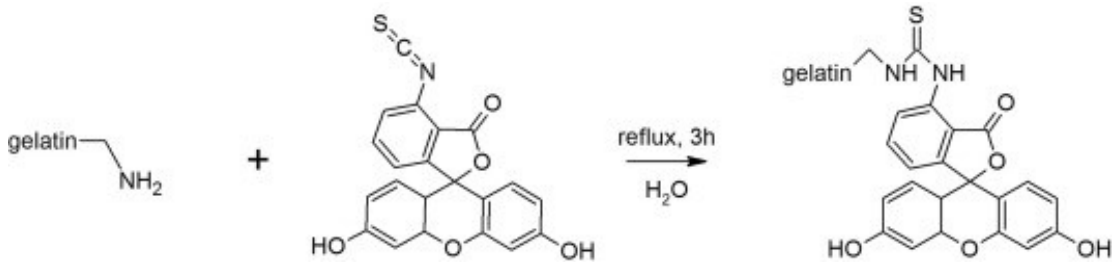

Figure 10. Reaction mechanism between FITC and gelatin [54]

It was observed that the addition of IRGACURE 2959 PI (blue curve) slightly stabilized the FITC-dextran fluorescence. It is speculated that free-floating FITC detached from dextran could complex with the IRGACURE 2959 via a mechanism similar to that on the –OH group of dextran (Figure 11). Although FITC-dextran is quite stable, this is a side reaction that may help improve fluorescence by converting the fluorophore into a state that causes less collisional quenching.

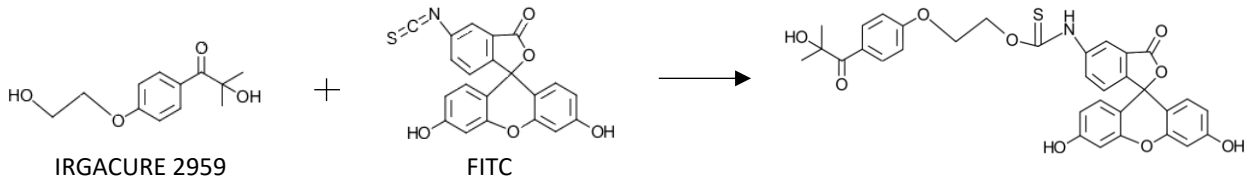

Figure 11. Proposed mechanism of FITC reaction with IRGACURE 2959

As the difference between GelA solution in PBS with and without PI was small, PBS (without PI) was used for future calibration curves. This medium was preferred over the solution with PI to avoid any potential cross-linked GelMA that may be formed in the UV irradiation step.

The precise cause of diminished fluorescence due to these reagents is still undetermined and may warrant investigation in the future. Conjugation of FITC-dextran with one of the reagents was unlikely due to its stability, however, a shielding effect caused by other reagents could have been present.

3.0.3 Effect of GelMA impurities

Centrifugation during the GelMA fabrication procedure was performed to remove any by-products (including unreacted MA and methacrylic acid [55]) that may still reside in the solution. These by-products have previously demonstrated toxic behaviour to cells [45], inhibiting cell growth onto GelMA materials. It had not been determined if these impurities affected the controlled release or loading of the 70kDa FITC-dextran and thus an investigation was conducted.

70kDa FITC-dextran loaded 10H- GelMA samples (centrifuge step removed) were created as an exaggeration to observe if the by-products influenced the fluorescent reading of FITC-dextran. The rationale behind this experiment was to determine if the purification steps during GelMA fabrication could be ignored to increase the throughput of GelMA material. Samples were created using either GelMA that was centrifuged and dialyzed for 7 days (GelMA) or one with the centrifuge step removed (impure GelMA). The samples were degraded overnight in $100 \mu g/mL$ MMP-9 and quantified (Figure 12).

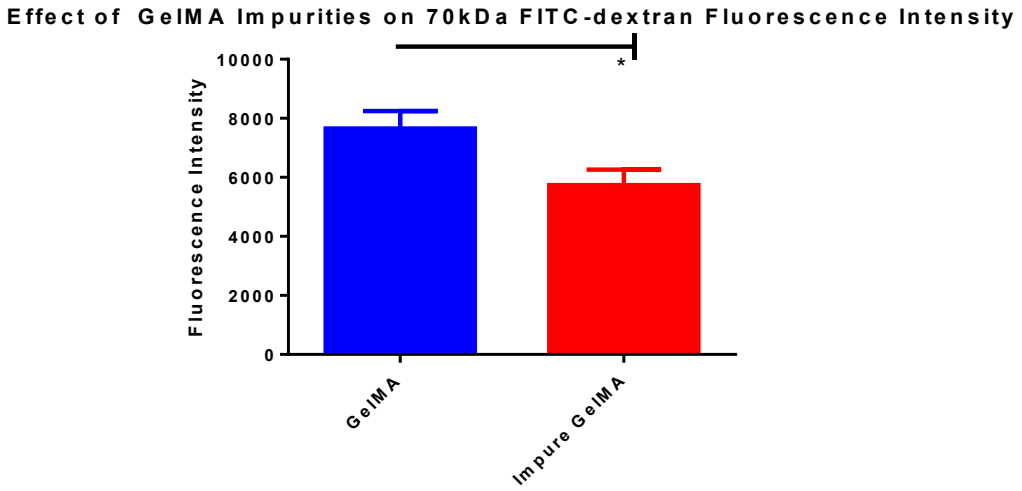

*Figure 12. Effect of GelMA impurities on 70kDa FITC-dextran fluorescence intensity (n=3). Error bars shown are SD. *:p<0.05*

Incorporation of GelMA impurities resulted in a significant 25% decrease in fluorescence intensity ($p<0.05$). As this variance was substantial, the week-long purification step was retained in the fabrication procedure. These results demonstrated the importance of both the centrifugation step and the dialysis step in order to remove any remaining impurities found in the GelMA solution.

The mechanism behind the quenching from the impurities is not well known, however, turbidity is a well-studied phenomenon that is known to decrease fluorescence intensities [47]. There is little information on how turbidity causes quenching, however, it is known that a large number particles (generally invisible to the naked eye) produces a decreased in fluorescent signal [47].

These experiments were performed to investigate the various parameters that may contribute to photo-quenching of the model molecule FITC-dextran. Although several factors (UV and controlled release reagents) negatively influence the fluorescence, FITC-dextran was used as the model molecule due to its cost efficiency and ease-to-quantify. A fluorescence stabilizer was not incorporated to reduce the amount of quenching as the controlled release studies were performed as a proof of concept to the profile of the drug to-be-delivered in GelMA. During the controlled release experiment of the actual drug used for corneal wound assays, an ELISA kit was used to quantify the actual amount released.

3.1 Controlled Release in GelMA

Controlled release studies were performed using either 10L-, 20L-, 30L-, 10L+, 20L+, 30L+, 10H-, 20H-, 30H-, 10H+, 20H+, or 30H+ GelMA patches. The 10, 20, and 30 represent the concentration of GelMA that was solubilized in the IRGACURE 2959 PI solution (% w/v), "H" and "L" signify a high and low methacrylation degree of GelMA, respectively, and a "+" suffix denotes an additional physical crosslinking step, whereas "-" represents a single UV irradiation crosslinking. These parameters were modified in order to obtain a foundation on the release characteristics from a GelMA hydrogel under the influence of MMP enzymes.

A FITC-dextran calibration curve was created prior to every controlled release experiment to quantify the amount of FITC-dextran that was released during each respective experiment. The concentrations of FITC-dextran that were used in the curve was calculated based on the theoretical amount (in μg) loaded in a single punched out cylinder of crosslinked GelMA. This value was

then multiplied by the concentration of FITC-dextran in the precursor solution to obtain the theoretical weight of drug loaded. The following calculation is an example for a 6mm diameter cylinder:

$$V_{cylinder} = \pi r^2 h$$
$$V = 3.1415926 * (3mm)^2 * (0.5mm)$$
$$V = 14.1371667mm^3$$
$$C_{loaded} = 14.1371667mm * \frac{0.001\ mL}{1\ mm^3} * 5\frac{mg}{mL}$$
$$C_{loaded} = 0.0706858335mg$$
$$C_{loaded} \cong 70.69\mu g$$

One primary issue that was previously demonstrated with FITC-dextran as a model molecule in a UV-irradiated hydrogel is its sensitivity to quenching, which caused an observed total release of 1%-60% of the theoretical loaded amount (~$70\mu g$) depending on the UV dosage in the controlled release studies. This established that a UV irradiated calibration curve containing similar reagents was not sufficient for mimicking the actual release profile. Additional factors in the controlled release study influenced the reading of the patches such that a 100% loading was not observed. It should be noted that although the true quantity of FITC-dextran cannot be determined, the values shown in each curve were proportional to the actual amount released. It was assumed that the molecule of interest would have a similar release profile.

The theoretical amount loaded was also calculated based on a homogeneous solution, that is, the FITC-dextran was evenly distributed within the mixture. Previous studies [56, 57] have demonstrated that dextran and gelatin form an incompatible solution, causing phase separation and dextran- or gelatin-rich domains. Although our solution was vortexed to improve homogeneity prior to crosslinking, the subsequent centrifuge step may cause further inconsistency in polymer distribution due to differences in molecular weight. The additional time required in the $60°C$ to reverse physical crosslinking may also allow for phase transition to occur prior to UV irradiation. It is recommended that in future experiments, the centrifuge time and speed be optimized to reduce the phase transition that occurs prior to UV crosslinking.

As previously mentioned, the concentration of MMP-9 enzyme present during several corneal diseases have been reported to be in the low hundreds of ng/mL; therefore, to mimic the

environment of the tear film, a concentration of 250ng/mL was used during the controlled release experiments. The error bars for the controlled release figures only included the lower standard deviation in order to improve clarity.

3.2.1 Physical Crosslinking

3.2.1.1 Effect of Polymer Concentration, Methacrylation on Physical Crosslinking

This experiment was performed to determine the degree of methacrylation required to have a steady release of 70kDa FITC-dextran over the course of 5-7 days. A controlled release study using low and high methacrylated 6mm diameter GelMA patches was performed and the release kinetics and time of degradation in $1\mu g/mL$ MMP-8 were observed (Figure 13). As MMP-8 enzyme degrades gelatin at a faster rate than MMP-9 (and also exists in the tear film) [58] [59], it was utilized during this controlled release experiment to represent a worst case scenario.

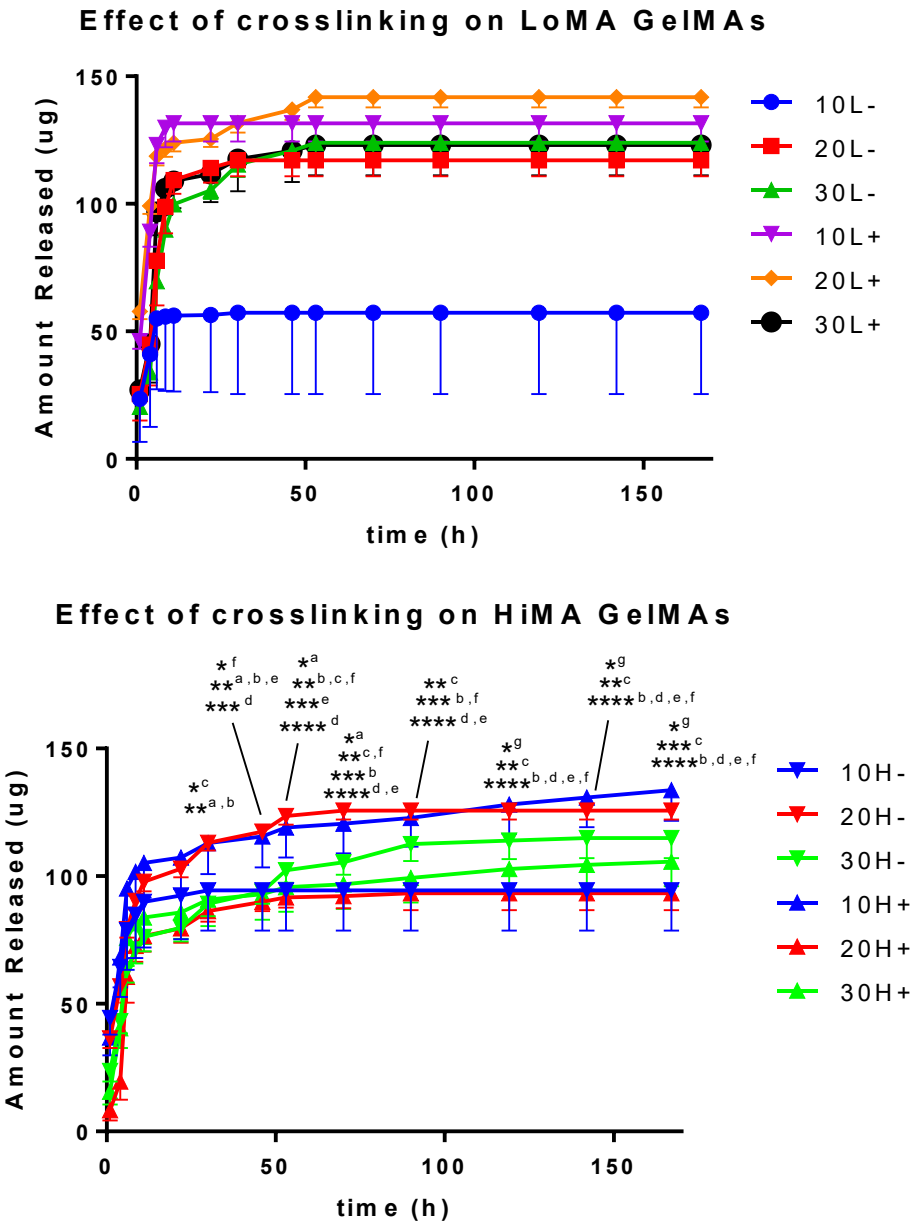

*Figure 13. Effect of concentration, methacrylation and crosslinking of GelMA degraded in 1µg/mL MMP-8 on controlled release of 70kDa FITC-dextran reading (n=4). LoMA = Low methacrylated, HiMA = High methacrylated, a – 20H- VS 30H-; b – 10H+ VS 20H+; c – 10H+ VS 30H+; d – 20H- VS 20H+; e – 10H- VS 20H-; f – 10H- VS 10H+; g – 10H- VS 30H-. ****: p<0.0001; ***:p<0.001; **:p<0.001; *:p<0.05 Error bars shown are SD.*

Regardless of the concentration of GelMA and additional physical crosslinking step, the low methacrylated samples fully degraded within three days and therefore were not suitable for RCE applications. These samples were also fragile and difficult to handle.

As the highly methacrylated samples demonstrated a wider range in degradation time, they were used for future experiments. The increased methacrylation degree provided a higher amount of crosslinking sites between the methacrylate anhydride, allowing for a slower breakdown of the gel within an MMP-rich environment. Similarly, the additional physical crosslinking step in "+" samples provided extra structural support allowing for a longer enzymatic cleavage time. The sequential crosslinking also reduced the pore size [60], creating an environment that was difficult for the drug to permeate through the membrane, thereby causing a lower burst release. After the initial burst release (first 24 hours), this effect was evident in the 20H- and 20H+ showing a significant change from the 46-hour until the end of the experiment ($p<0.001$ for 46-hour and $p<0.0001$ for rest of time points). This was also demonstrated between the 10H- and 10H+ samples at the same time points ($p<0.05$ at 46-hour, $p<0.01$ from 53-70 hour, $p<0.001$ at 120-hour and $p<0.0001$ until the rest of the experiment. A higher concentration of GelMA demonstrated a denser polymer matrix inside the gel which significantly reduced the rate of diffusion of FITC-dextran to the external environment [60]. This effect was demonstrated in the non-physically crosslinked samples such as the 20H- and 30H- samples from the 30-70 hour ($p<0.01$ from 30-46hour and $p<0.05$ from 53-70 hour); 10H- and 20H- from 46-hour until end of experiment ($p<0.01$ at the 46-hour, $p<0.001$ at the 53 hour and $p<0.0001$ from the 70-hour until the end of the experiment); 10H- and 30H- from 120-hour until the end of experiment ($p<0.05$). The samples with an additional physical crosslinking step also displayed a concentration dependent release, showing a significant different between the 10H+ and 20H+ samples from the 30-hour until the end of experiment ($p<0.01$ from the 30-53hour, $p<0.001$ from the 70-90 hour, and $p<0.0001$ from the 120-hour until end of experiment); as well as between the 10H+ and 30H+ samples at the 30-hour mark and between the 53-hour until the end of experiment ($p<0.05$ at the 30-hour, $p<0.01$ from 53-142 hour and $p<0.0001$ at the 167-hour).

A similar experiment under the influence of 250ng/mL MMP-9 was also examined using the highly methacrylated GelMA material (Figure 14).

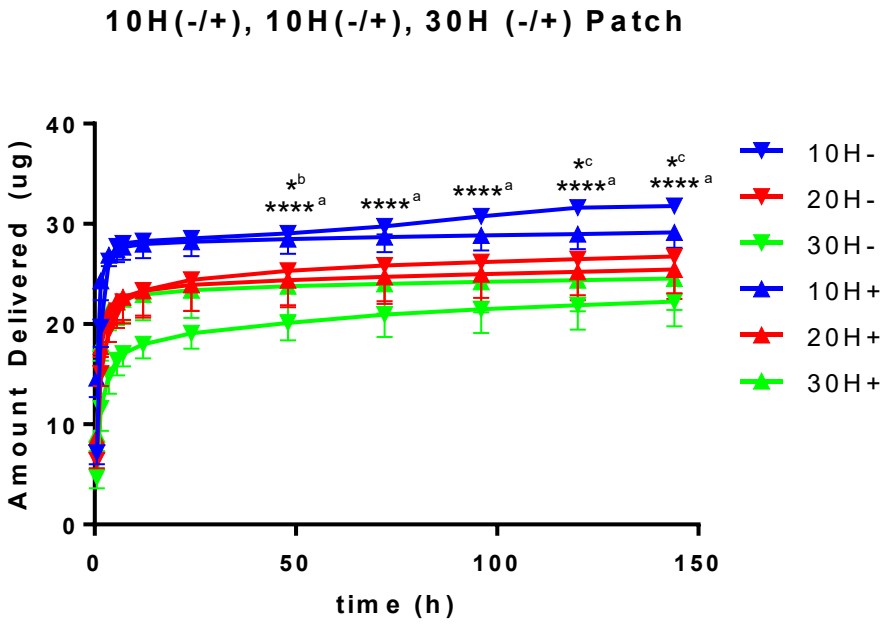

*Figure 14. Effect of concentration, methacrylation and crosslinking of GelMA degraded in 250ng/mL MMP-9 on controlled release of 70kDa FITC-dextran (n=19). a – 10H- VS 30H- b – 20H- VS 30H-; c – 10H- VS 20H-. ****:p<0.0001; *:p<0.05. Error bars shown are SD.*

A higher concentration of GelMA resulted in a lower burst release of FITC-dextran. It was shown that after the initial burst release (first 24 hours), the 20H- showed a significantly higher release than the 30H- at the 48-hour ($p<0.05$). The 10H- additionally demonstrated a faster release between the 122- and 144-hour ($p<0.05$). The 10H- showed a significantly quicker release over the 30H- patches from the 1.5-hour until the end of the experiment ($p<0.0001$). It was demonstrated that the physical crosslinking step did not reduce the burst release rate as it had with the MMP-8. According to Huang et al., burst release in hydrogels is caused by: processing conditions, surface characteristics of host material, sample geometry, host/drug interactions (surface adsorption), and morphology and porous structure of dry material. As all these parameters were identical in both of the experiments, the outlying difference are the enzyme types. It is speculated that the cause is due to the different mechanisms of peptide cleavage between MMP-9 and MMP-8 [61].

3.2.1.2 Effect of UV Dosage on Physical Crosslinking

This experiment compared two UV crosslinking machines that possessed different power and wavelengths. GelMA patches of concentrations 10H-, 20H-, 30H-, 10H+, 20H+, and 30H+ were

loaded with 70kDa FITC-dextran and UV irradiated for 300s using either the 265nm FB-UVXL-1000 UV crosslinker, or the 365nm HTBX UVLED oven (Figure 15 and).

The UV dosage can be represented in mJ/cm^2 by multiplying the power of the crosslinker by the time the sample was irradiated. A sample calculation of the HTBX UVLED at 600mW/cm^2 is provided:

$$600\frac{mW}{cm^2} * 300s = 180{,}000\frac{mW * s}{cm^2}\ , where\ 1\ mW * s = 1mJ$$

$$\therefore UV\ dosage = 180{,}000\frac{mJ}{cm^2}$$

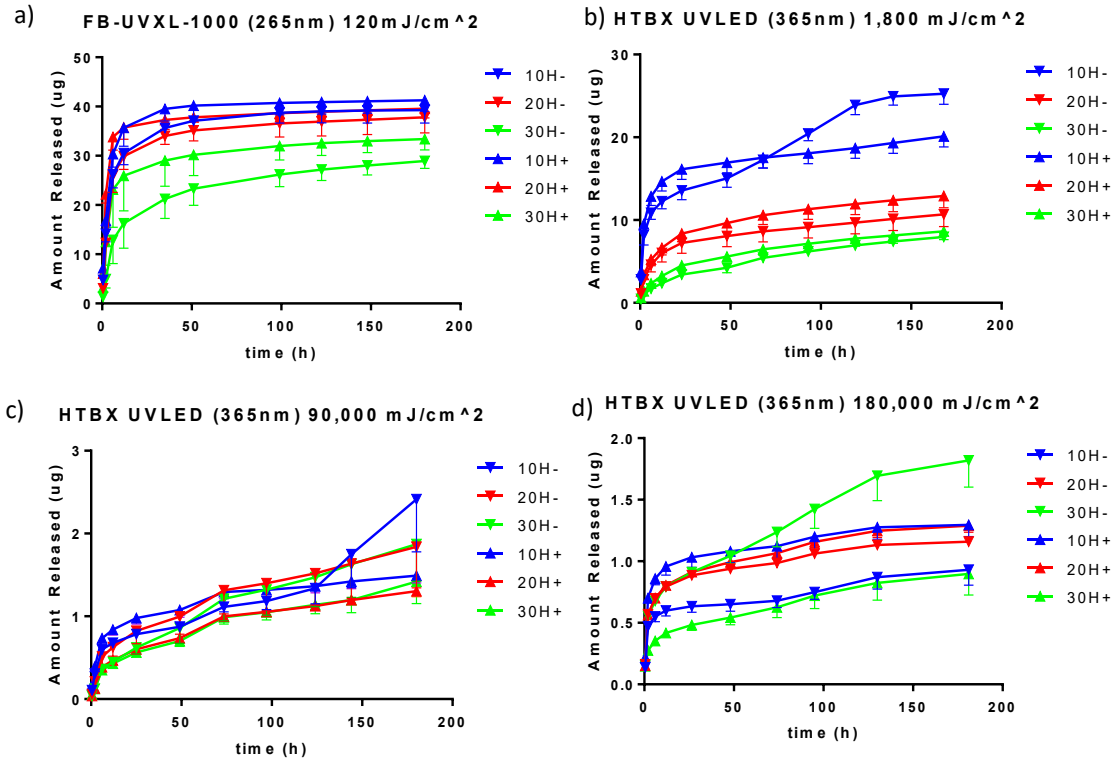

Figure 15. Effect of UV dosage on various concentration and optional physical crosslinking step of GelMA controlled release of 70kDa FITC-dextran (n = 3). Error bars shown are SD.

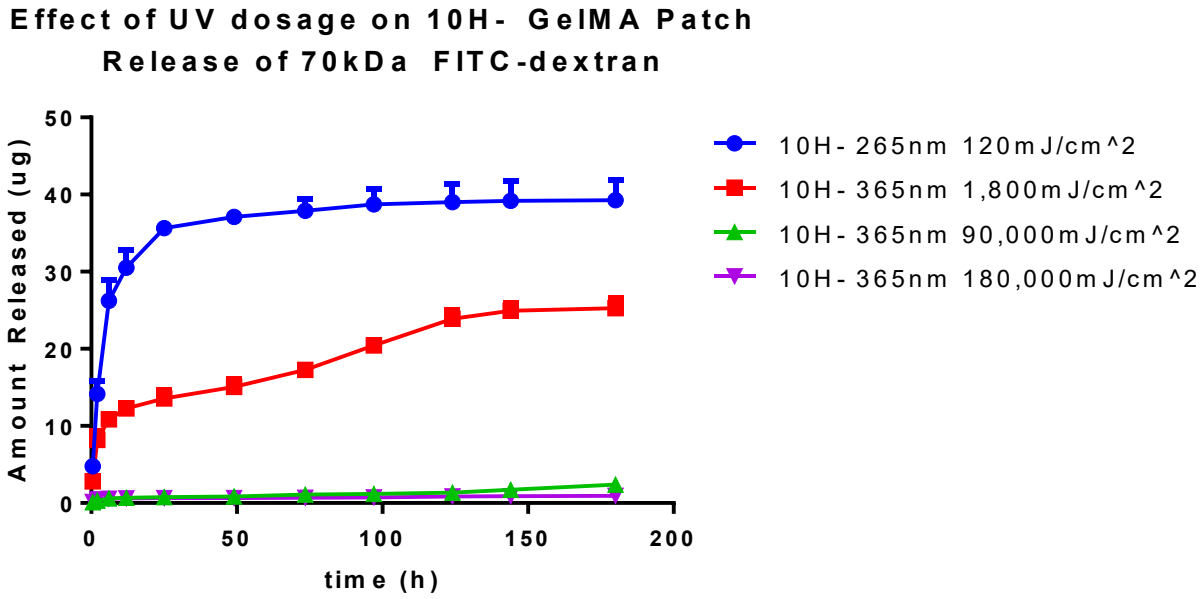

Figure 16. Effect of UV dosage on 10H- GelMA controlled release of 70kDa FITC-dextran (n = 3). Error bars shown are SD.

It was demonstrated that a UV dosage of 180,000, 90,000, and 1,800 mJ/cm^2 at 365nm wavelength (Figure 15b,c,d) released different orders of magnitude FITC-dextran due to the varying dosage of UV irradiation. This effect is better visualized in Figure 16, which exemplifies the significance of the UV dosage on the observed 10H- FITC-dextran readings. After the initial burst release (first 24 hours), the effect of UV dosage was significant between all 10H- samples ($p<0.0001$) from the 25-hour until the end of experiment except between the 90,000mJ/cm^2 and 180,000mJ/cm^2-irradiated samples, which showed no significant change. The fluorescence of the FITC-dextran was severely extinguished following the 180,000mJ/cm^2 and 90,000mJ/cm^2 UV irradiation wherein the GelMA samples became completely white (the natural colour of the GelMA), causing a low release percentage of the theoretical amount loaded.

The 10H- GelMA samples irradiated with 1,800 mJ/cm^2 of 365nm UV and 120mJ/cm^2 of 265nm UV were visibly completely degraded by the 250ng/mL MMP-9 by the 120-hour mark. Although this is not apparent from Figure 14b, it is speculated that the continued release was due to excess FITC-dextran that remained at the bottom of the well-plate. The 180,000mJ/cm^2 and 90,000mJ/cm^2 10H- samples, on the other hand, were fully present on day 7. This suggested that a UV dosage of 1,800mJ/cm^2 at 365nm and 120mJ/cm^2 at 265nm could not provide a gel robust enough to release FITC-dextran over the course of 7 days.

This posed conflicting future steps as a higher and longer UV exposure were required for a longer lasting gel, however, the FITC-dextran was not sustainable under strong UV irradiation. Although FITC-dextran was simple to quantify using a plate reader, a different model molecule could be considered or, a new crosslinking method for GelMA could be experimented upon (thermal crosslinker instead of UV) for future experiments. For simplicity, FITC-dextran and a higher UV dosage were utilized to predict the release profile of actual drug in a wound assay.

This section evaluated the effects of tuning methacrylation degree, concentration of GelMA, and UV dosage on the controlled release profile of GelMA. Increasing the methacrylation degree allowed for additional crosslinking sites upon UV irradiation and proved to increase the lifespan of the gel within an MMP-rich environment to the 5-7 day targeted release length. A higher concentration of polymer resulted in a denser polymer matrix which reduced the permeability of 70kDa FITC-dextran through the membrane and therefore providing a lower burst release. Similarly, adding a physical crosslinking step reduced the pore size of the GelMA whilst providing a structural stronger gel that limited the diffusion of drug to the external environment. This effect was notable in MMP-8, but not MMP-9 due to the different cleavage mechanism of the enzymes.

3.1.1 Effect of Concentration of MMP Enzyme (MMP-8) and Size of Molecule

As an additional physical crosslinking step reduced the pore size of the hydrogel and an increased polymer concentration minimizes drug permeability through the gel matrix, an experiment examining the molecular weight cut-off of FITC-dextran in GelMA was conducted. GelMA patches loaded with either 4kDa (Figure 17) or 70kDa FITC-dextran (Figure 19) were dissolved in PBS or PBS solutions containing $1\mu g/mL$ MMP-8. An additional $50\mu g/mL$ sample was run in parallel to confirm that MMP-8 played a role in degradation of GelMA. The significance between the 20H+ and 30H+ in either PBS, 1 μg/mL MMP-8, or 50 μg/mL MMP-8 was illustrated in Figure 20.

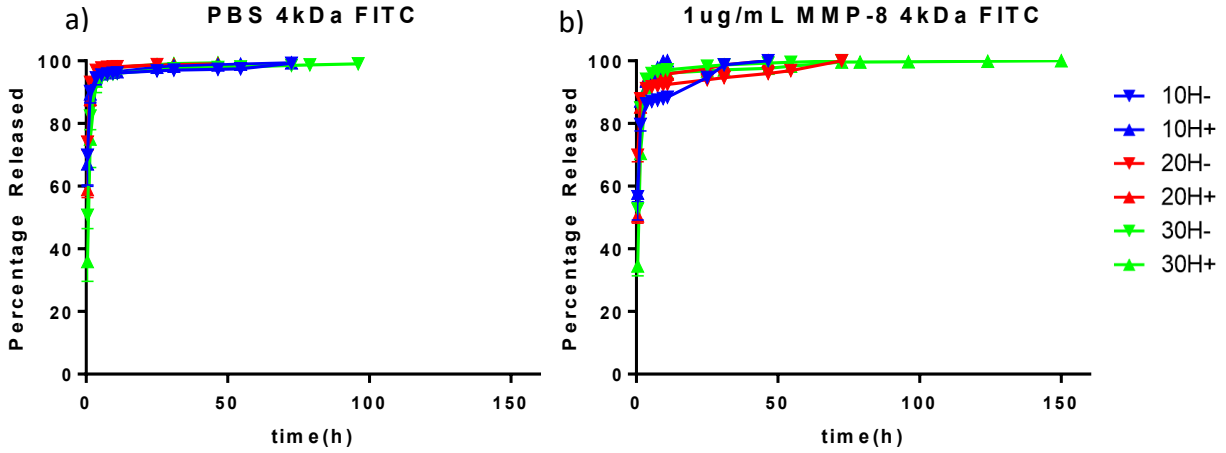

Figure 17. Effect of PBS and 1µg/mL MMP-8 enzyme on controlled release of 4kDa FITC-dextran from varying concentrations and optional physical crosslinking step of GelMA (n=4). Error bars shown are SD

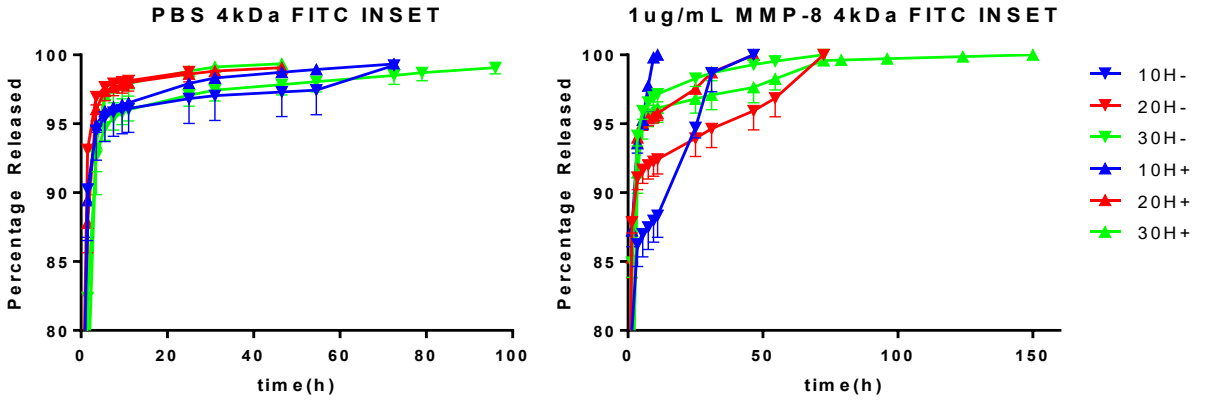

Figure 18. Inset of Figure 17 demonstrating the release profile between 80-100% on effect of PBS and 1µg/mL MMP-8 enzyme on controlled release of 4kDa FITC-dextran from varying concentrations and optional physical crosslinking step of GelMA (n=4). Error bars shown are SD.

The percentage released was calculated as opposed to amount of drug released in order to demonstrate the completion of the controlled release (when no more drug was delivered). The 4kDa FITC-dextran completely eluted from the hydrogel within the first 3 days despite the presence of MMP-8 enzyme and concentration of GelMA (Figure 17) revealing that the drug is able to more freely permeate through the gel despite the smaller pore size from the "+" physical crosslinking. Ignoring the initial burst release (first 24 hours), only the 20H- sample demonstrated a significant variation in 4kDa FITC-dextran release from the 31-55 hour ($p<0.0001$ from 31-47hour and $p<0.001$ from 47-55 hour) In comparison, the 70kDa FITC-dextran demonstrated a stronger concentration- and physical crosslinking-dependent release profile, resulting in a more controllable enzyme-mediated release.

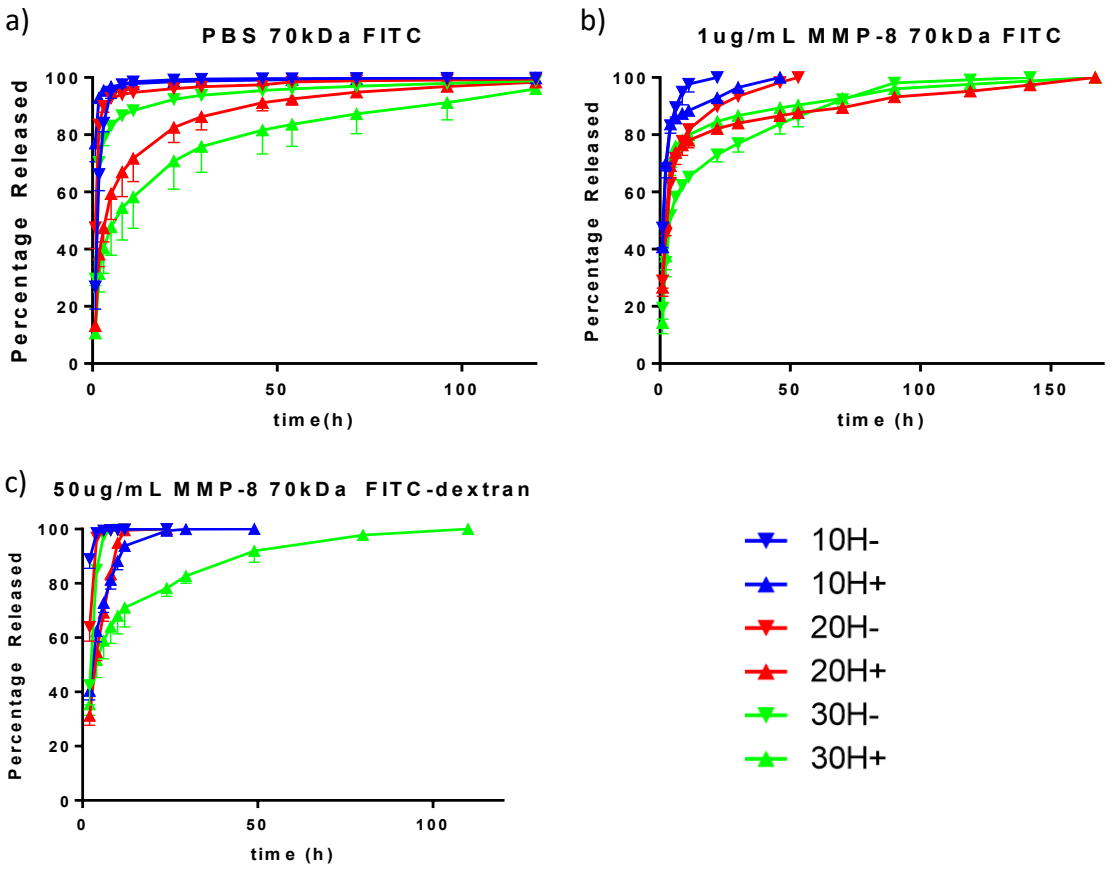

Figure 19. Effect of PBS, 1µg/mL and 50µg/mL MMP-8 enzyme on controlled release of 70kDa FITC-dextran in various concentrations and optional physical crosslinking step from GelMA (n=4). Error bars shown are SD

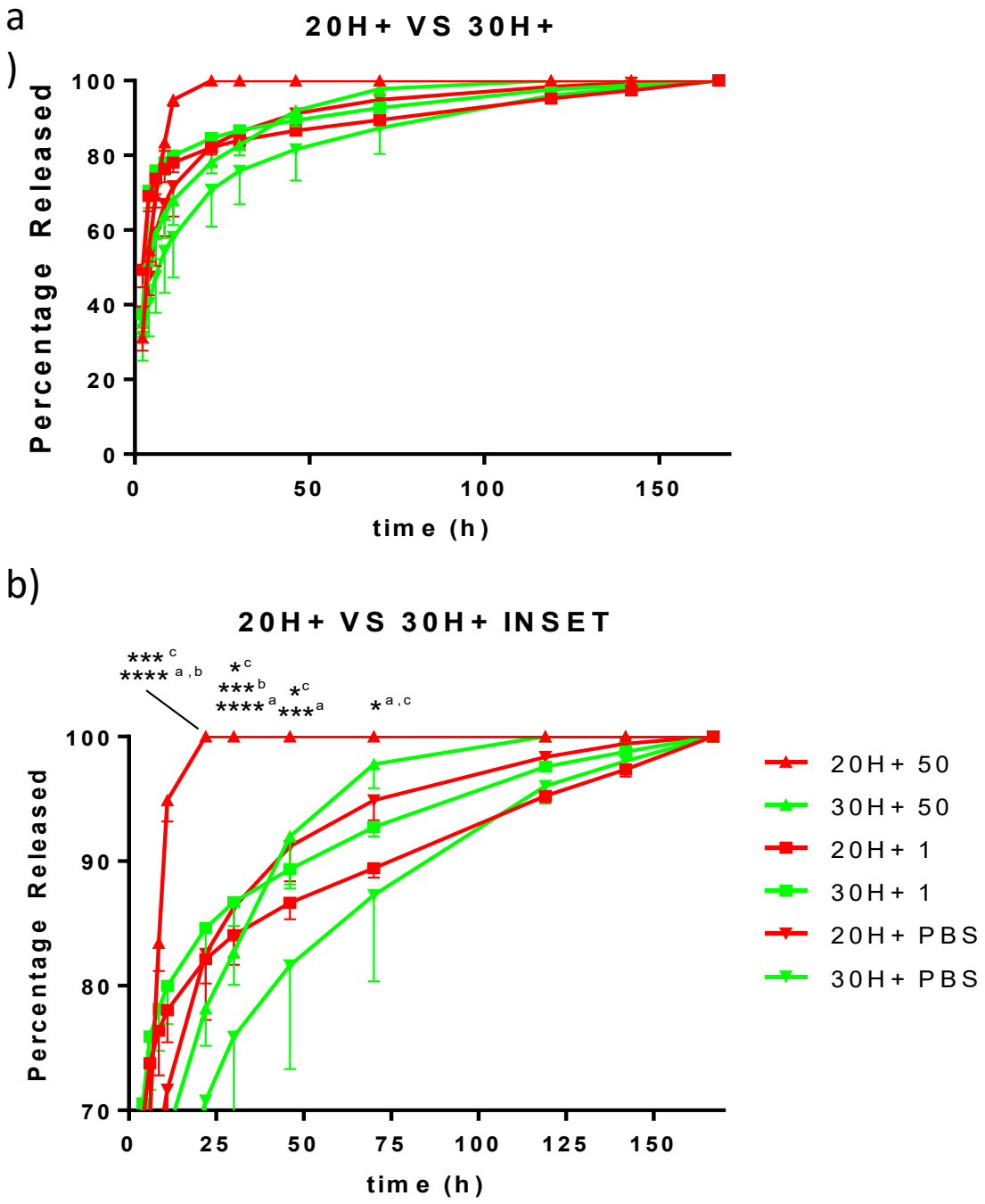

*Figure 20. a) Effect of PBS, 1µg/mL and 50µg/mL MMP-8 enzyme on 20H+ and 30H+ GelMA controlled release of 70kDa FITC-dextran (n=4). b) Inset of image a) depicting release profile after initial burst release (~75% within 24 hours). a – 20H+ in 50µg/mL MMP-8 VS 1µg/mL MMP-8; b – 20H+ 50 µg/mL MMP-8 VS PBS; c – 30H+ 1 µg/mL MMP-8 VS PBS. ****:p<0.0001, ***:p<0.001, *:p<0.05 Error bars shown are SD*

The concentration of MMP-8 enzyme proved to be a major contributor to the enzymatic degradation of the hydrogel as demonstrated by the release profile in Figure 19. After the initial

burst release (first 24 hours), the 20H- samples degraded in $50\mu g/mL$ were significantly different than that of the $1\mu g/mL$ ($p<0.005$) and PBS ($p<0.05$) samples at the 30-hour. The 30H- GelMA patches from the 50- and $1\mu g/mL$ samples were significantly slower than the PBS ($p<0.0001$ and $p<0.01$, respectively) 30H- sample from the 46-70 hour. The 10H+ degraded in $50\mu g/mL$ was degraded significantly quicker than the 10H+ in $1\mu g/mL$ ($p< 0.0001$), which, in turn, was significantly faster than the PBS 10H+ ($p< 0.0001$) sample from the 30-hour until the 119-hour. It is demonstrated from Figure 20b that the 20H+ degraded in $50\,\mu g/mL$ MMP-8 had a significantly different release rate from an identical patch in $1\mu g/mL$ MMP-8 from the 22-90 hour ($p<0.0001$ from 22-30 hour, $p< 0.001$ at 46-hour and $p<0.05$ at the 70-hour mark). It was additionally shown that the 20H+ degraded in $50\,\mu g/mL$ MMP-8 released FITC-dextran significantly faster than the equivalent PBS sample between the 22- and 30-hour ($p<0.0001$ and $p<0.001$, respectively). The 30H+ degraded in $1\mu g/mL$ MMP-8 demonstrated a significantly faster release over the 30H+ in PBS from the 22-30hour ($p<0.001$ at the 22-hour and $p<0.05$ at the 30 hour). The 30H+ degraded in $50\mu g/mL$ possessed a release rate significantly faster over the corresponding PBS sample between the 46-70 hour ($p<0.05$).

These results indicated that the MMP-8 enzyme played a key role in the release profile of the hydrogels. It also revealed that 4kDa molecules were below the threshold that GelMA could load and they were able to freely permeate without obstruction, implying a diffusion-limited release. Using this information, it is recommended in future experiments that a 30H+ GelMA is used (to limit permeability inside the gel as well as to reduce the porosity) in combination with a higher molecular weight molecule in order to minimize burst release and have an enzyme-mediated release.

3.1.2 Effect of Enzyme Type (MMP-8 VS MMP-9) (CL and Patch)

As previously mentioned, MMP-8 and MMP-9 cleave gelatin differently. In order to differentiate the release profile between MMP-8 and MMP-9, the enzymes were compared. An experiment degrading a 4mm GelMA-loaded Biofinity CL or a 6mm pure GelMA patch was performed over 5 days using $1\mu g/mL$ of either MMP-8 or MMP-9 (Figure 21).

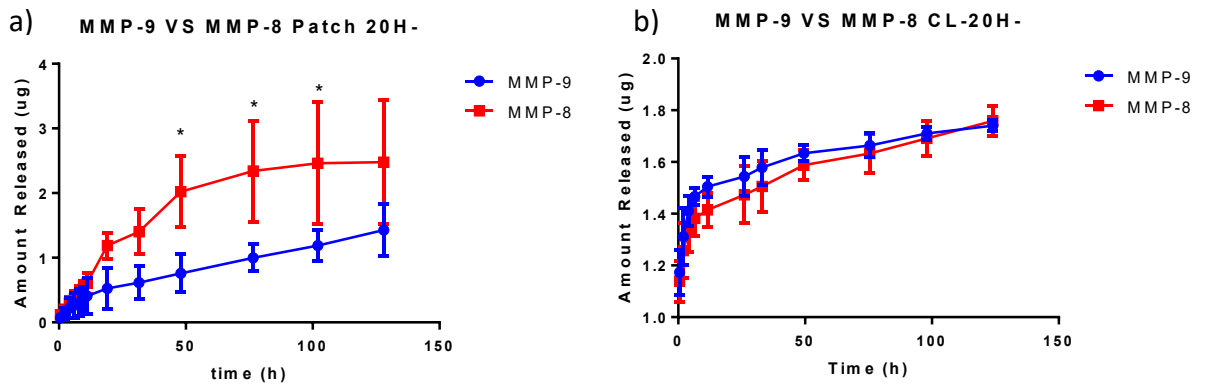

Figure 21. MMP-8 VS MMP-9 enzyme on 20H- GelMA patch and 20H- GelMA-incorporated CL release of 70kDa FITC-dextran (n=9). Error bars shown are SD.:p<0.05*

An interesting phenomenon occurred where the GelMA patches degraded in MMP-8 (Figure 21a) released 70kDa FITC-dextran significantly faster than ones in MMP-9 as shown by an increased release of 166%, 134%, and 107% at the 48-, 77- and 102-hour. This effect was not significant at any time point when the GelMA was incorporated in a CL (Figure 21b). This suggested that the CL and acts as a larger barrier to MMP-8 over MMP-9 due to their specific cleavage sites of the hydrogel [61]. Since RCE is primarily caused by MMP-9 enzyme [13], future experiments focused on this enzyme, however, as several MMP enzymes are present in the tear film during RCE [62], it is advised that the effect of each enzyme at physiological concentrations on GelMA degradation is investigated.

Reflecting on the controlled release studies, despite the quenching of FITC-dextran, the model molecule provided an accurate prediction of the release profile for the molecule selected (discussed later). Highly methacrylated GelMA was chosen over low methacrylation as it demonstrated a large tunable profile within the 5-7 day range based on concentration of GelMA dissolved in PBS solution containing PI.

3.1.3 Optimization of GelMA Patch

Experiments were performed in an attempt to optimize the controlled release profile of a 70kDa drug from a GelMA patch. These studies were performed to achieve a different release pattern in order to satisfy an accelerated corneal epithelial wound healing. An explanation for the design process behind the mechanism is provided.

3.1.3.1 Patterning of Patch

Patterning the surface of a 6mm GelMA patch was investigated to accelerate the release of drug. The rationale behind this study was to increase the surface area that the drug may diffuse from the hydrogel as depicted in Figure 22. Any pattern that is added to the surface of the hydrogel would increase the surface area, which would theoretically accelerate the release of drug. The patterns implemented on the surface of the hydrogel for this experiment were 900nm pillars that were spaced approximately 900nm apart. As these patterns were from a previous lab, the height of these features is currently unknown. The presence of the pillars on the GelMA patch were confirmed with phase contrast microscopy. Alternate patterns may be investigated for various controlled release profiles, however, 900nm pillars were chosen as a proof of concept.

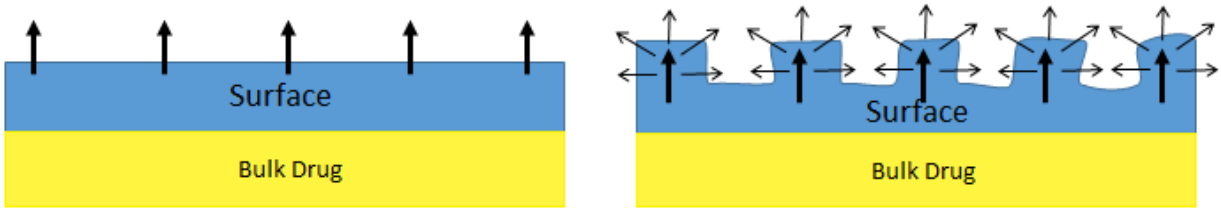

Figure 22. Schematic of proposed patterning mechanism on surface of GelMA

The GelMA patch was loaded with 70kDa FITC-dextran and the controlled release profile was calculated (Figure 23). These hydrogels were soaked in PBS *without* MMP enzyme to ensure that the pattern on the surface remained intact (to demonstrate that the change in release profile was solely due to the increased surface area and not the presence of MMP enzyme).

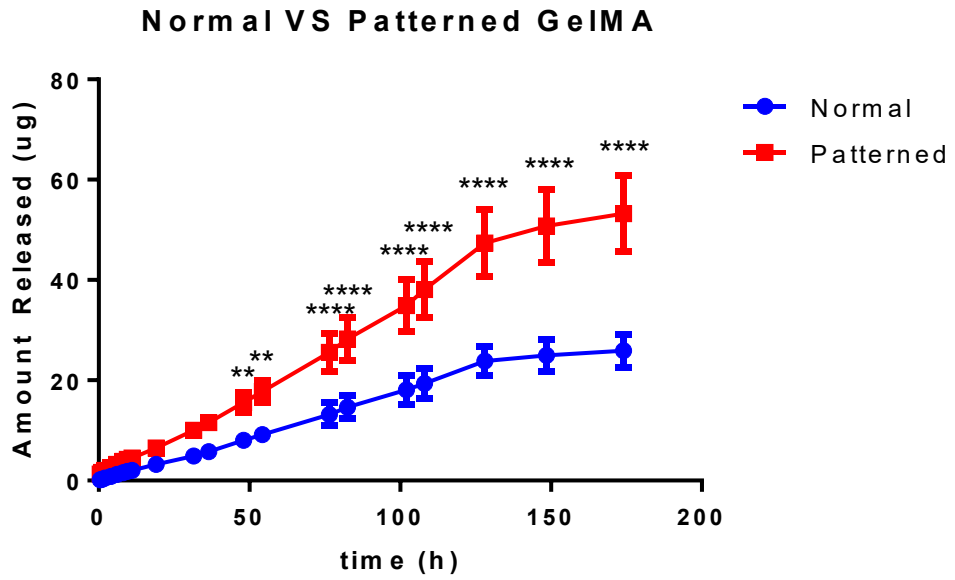

*Figure 23. Effect of patterning 20H- GelMA patch on controlled release profile of 70kDa FITC-Dextran (n=4). Error bars shown are SD. **:p<0.01, ****:p<0.0001*

The GelMA patch demonstrated an average of 2.47 times the amount of FITC-dextran released (the first 24 hours were not included in this calculation as it was burst release) over the course of seven days in PBS solution. The amount of increased surface area due to the patterns was calculated to determine if this was the underlying cause of the accelerated release rate. The surface area of the 6mm GelMA patch that is releasing drug is that of a cylinder minus one side (as this side is in contact with the bottom of the well-plate, it is assumed that no drug leaves from this surface).

$$Surface\ area\ of\ cylinder\ missing\ a\ side = 2\pi rh + \pi r^2$$

$$\therefore SA_{unpatterned} = (2 * 3.14159 * 3mm * 0.5mm) + (3.14159 * (3mm)^2)$$

$$SA_{unpatterned} = 9.42477mm^2 + 28.27431mm^2$$

$$SA_{unpatterned} = 37.69908mm^2$$

The surface area gained from each 900nm feature can be determined by calculating the wall of each pillar. Assuming the height of the pillar was 1 micron, this equate to:

$$Area\ of\ cylinder\ wall = 2\pi * r_{pillar} * h_{pillar}$$

$$\therefore\ SA_{added} = 2 * 3.14159 * 0.00045mm * 0.001mm$$
$$SA_{added} = 0.000002827431mm^2$$

As the pillars were spaced 900nm apart, we can place each pillar into a square to approximate the area representing one feature.

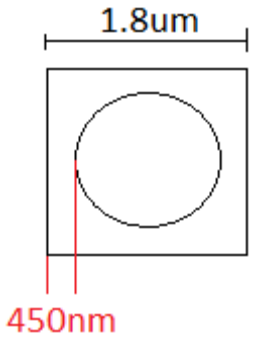

Figure 24. Diagram depicting one 900nm pillar feature

Where the area of the square is:

$$Area_{square} = 1.8\mu m * 1.8\mu m$$
$$Area_{square} = 3.24\mu m^2$$

The area of the 6mm GelMA hydrogel is:

$$Area_{GelMA} = 3.14159 * (3mm)^2$$
$$Area_{GelMA} = 28.27431mm^2$$
$$Area_{GelMA} = 28274310\mu m^2$$

Dividing these two areas will determine the number of pillar features there were:

$$Number\ of\ pillars = \frac{Area_{GelMA}}{Area_{square}}$$
$$Number\ of\ pillars = \frac{28274310\mu m^2}{3.24\mu m^2}$$
$$Number\ of\ pillars = 8726638.9$$

The number area surface area gained is then the accumulated surface area of each of these pillars:

$$SA_{increased} = 0.000002827431mm^2 * 8726638.9$$
$$SA_{increased} = 24.673969mm^2$$

And the new surface area can be calculated:

$$SA_{patterned} = 37.69908mm^2 + 24.673969mm^2$$

Thus, the ratio increased surface area is:

$$SA_{ratio} = \frac{SA_{patterned}}{SA_{unpatterned}}$$
$$SA_{ratio} = \frac{62.37305mm^2}{37.69908mm^2}$$
$$SA_{ratio} = 1.654$$

From these calculations, it appeared that the larger surface area only contributed to a portion of the increased release rate. Peer et al. [63] discovered that the significant change in surface properties from patterning is not the increased surface area, but rather the modification of wetting. It was revealed that topographies that induced a more hydrophobic surface decreased the release rate, whereas a more hydrophilic surface would accelerate increased the drug delivered. It is recommended that water contact angle measurements be performed on these surfaces to determine if the same trend is observed with the 900nm pillars on GelMA.

3.2 Wound Assay

Wound assays were used to verify the efficacy of HA and BLf in corneal epithelial wound healing. Investigations using both scratch wound assays (scratch wound assays) and PDMS wound assays (PDMS wound assays) were performed to examine the effect of different wound assays on the cell type and molecules. Primary RCEpCs were initially purchased as they would behave similar to that in future *in vivo* rabbit studies, however, later wound assays utilized SV-40 immortalized HCEpCs because they were easier to handle and as these cells were provided by a collaborator.

The error bars for each of the wound assay figures only included the lower standard deviation in order to improve clarity. A table presenting any significant improvement in wound healing is provided.

3.2.1 Refining of Wound Assay

A control (plain KM) was compared to that of media containing 2.5mg/mL BLf, 7.5mg/mL BLf, 0.45mg/mL HA, or 0.75mg/mL HA. These concentrations were initially added as a bolus dose to mimic previously cited conditions. Once an appropriate molecule was chosen, a PDMS wound

assay study was performed using a daily concentration of drug to imitate a controlled release system (section 3.2.2).

Previous literature on HA for corneal epithelial cells utilized either oligo-HA (<10kDa) or native (high molecular weight) HA [38, 39]. As 4kDa FITC-dextran immediately eluted from the GelMA patches, a low molecular weight drug was not viable and therefore a molecular weight HA of 500kDa was initially used for the preliminary wound assays.

3.2.1.1 RCEpCs Scratch Wound Assay

As RCE is commonly caused by mechanical trauma to the eye (as opposed to a chemical or alkaline burn) [64], an initial wound assay was performed using a scratch method. The experiment used two concentrations of either drug (Figure 25) in order to determine the therapeutic window.

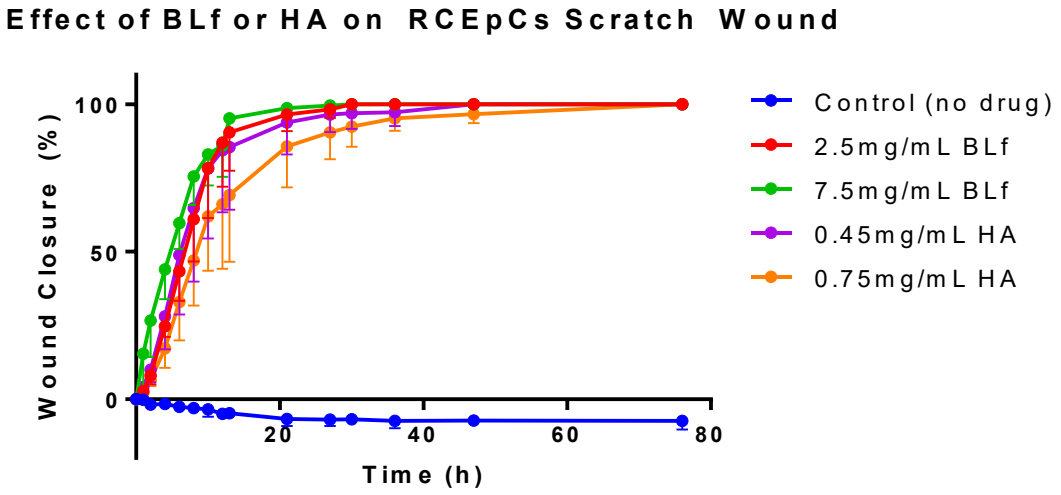

Figure 25. Effect of 2.5mg/mL bovine lactoferrin (BLf), 7.5mg/mL (BLf) 0.45mg/mL hyaluronic acid (HA), 0.75mg/mL HA versus control (no drug) in rabbit corneal epithelial cells (RCEpCs) scratch wound assay (n = 3). Error bars shown are SD

The control samples from the experiment did not recover and instead enlarged over the course of three days. It was difficult to quantify the increase in wound healing relative to the control as the abrasion never improved, however, all time-points were significantly faster versus the control from the 6th hour until completion ($p<0.001$).

An increase in drug concentration for BLf or HA did not demonstrate a significant increase in wound healing, however, a 7.5mg/mL BLf concentration healed faster than 0.75mg/mL HA concentration (Table 1). This effect remained throughout the 4-8 hour time points with a decrease in wound size from 155.7% at the 4-hour mark to 60.8% reduced size at the 8-hour mark.

Table 1. Significance between BLf and HA on RCEpCs scratch wound assay

Time (h)	Samples	Significance	% improved	P-value
4	7.5mg/mL BLf VS 0.75mg/mL HA	*	155.7%	0.0140
6	7.5mg/mL BLf VS 0.75mg/mL HA	*	81.2%	0.0141
8	7.5mg/mL BLf VS 0.75mg/mL HA	**	60.8%	0.0074

The wound area of the scratch wound assay varied drastically between samples as shown in Figure 26. Using Graphpad Prism, the standard deviation of the initial scratch wound area was calculated to be 12.2% (Figure 27). This variance in wound area was caused by human error based on the angle and pressure of the P200 tip while performing the scratch. It was also noted that as the wound size was larger than the obtainable captured image, it was difficult to quantify the wound area using ImageJ. It was for this reason that the scratch wound assay was discontinued and a PDMS wound assay method was adopted. Reflecting on these results, the scratch wound assay method is only an issue depending on the method of analysis. For example, if one were tracking individual cell migration, the variation in initial wound size would not cause complication. As a cell tracking set-up was not available, a PDMS wound assay method was utilized to quantify a more consistent initial wound size.

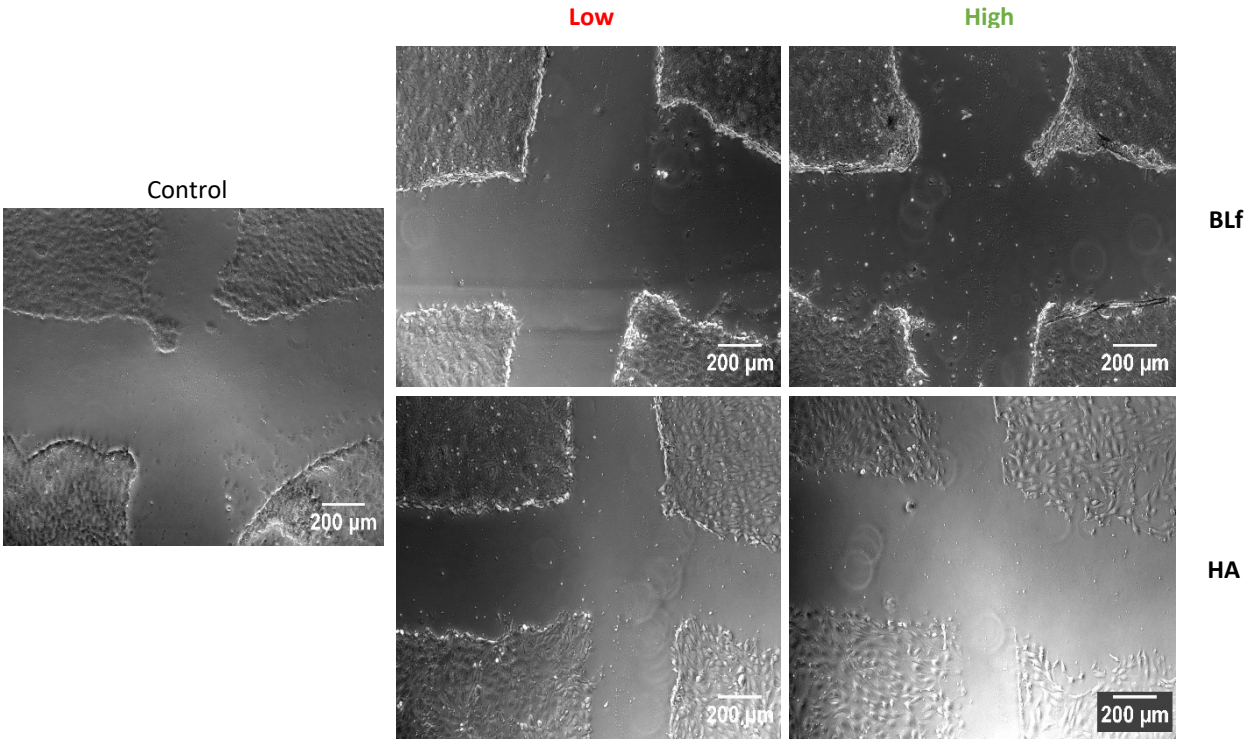

Figure 26. Phase contrast image of initial wound scratches using P200 pipette tip

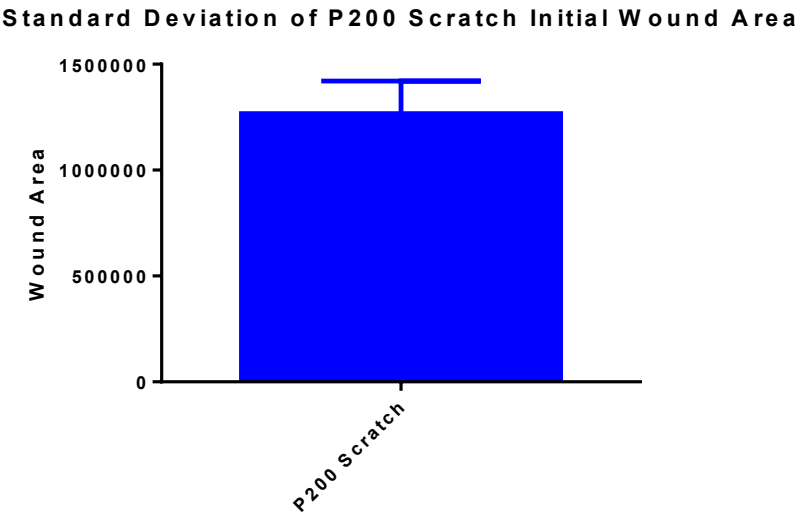

Figure 27. Standard deviation of initial wound area of scratch wound assay (n =15). Error bar shown is SD

3.2.1.2 HCEpCs 2mm PDMS Wound Assay

In this experiment, a PDMS wound assay was used to obtain a consistent initial wound area. Another benefit of a circular PDMS wound is the multi-directional migration for the cells as opposed to the linear migration resulting from scratch wounds to eliminate directional wound-healing bias [65]. A 2mm diameter wound was tested as it was the smallest diameter punch available, however, it was discovered that the wound created was too large for the lowest magnification to image. The results were recorded as best as possible and quantified (Figure 28).

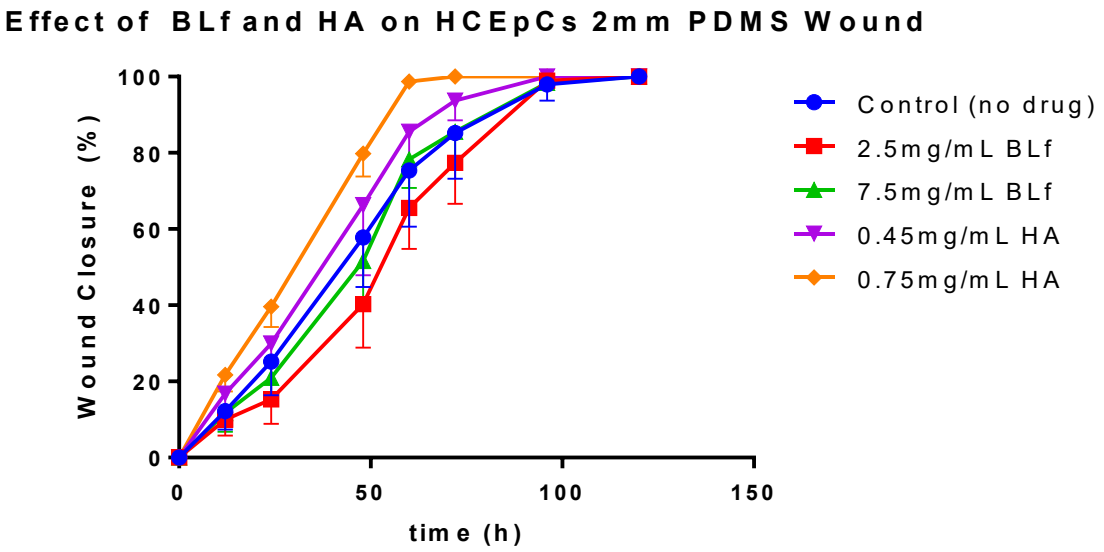

Figure 28. Human corneal epithelial cells (HCEpCs) 2mm PDMS wound assay (n = 5). Error bars shown are SD.

Comparing the concentrations of drug, a higher BLf concentration demonstrated a quicker wound healing at the 48- and 60-hour by 22.0 and 16.2%, respectively, whereas the 0.75mg/mL HA demonstrated a quicker wound closure over the 0.45mg/mL HA at the 48- and 60-hour by 22 and 13.4%, respectively. The 2.5mg/mL concentration of BLf showed a slower wound healing with a significantly larger wound area compared to the 0.45mg/mL HA (between the 24- and 60 hours) and 0.75mg/mL (between the 12-hour and 72 hour). Similarly, the 7.5mg/mL demonstrated a larger wound size compared to the 0.45mg/mL HA at the 48-hour and the 0.75mg/mL from the 24-hour to 72-hour.

Table 2. Significance between BLf and HA on HCEpCs 2mm PDMS wound assay

Time (h)	Samples	Significance	% improved	P-value
12	2.5mg/mL BLf VS 0.75mg/mL HA	*	-54.0%	0.0364
24	2.5mg/mL BLf VS 0.45mg/mL HA	**	-48.8%	0.0050
	2.5mg/mL BLf VS 0.75mg/mL HA	****	-61.3%	< 0.0001
	7.5mg/mL BLf VS 0.75mg/mL HA	***	-47.2%	0.0002
48	2.5mg/mL BLf vs. 7.5mg/mL BLf	*	-22.0%	0.0461
	2.5mg/mL BLf vs. 0.45mg/mL HA	****	-39.2%	< 0.0001
	2.5mg/mL BLf vs. 0.75mg/mL HA	****	-49.5%	< 0.0001
	7.5mg/mL BLf vs. 0.45mg/mL HA	**	-22.0%	0.0051
	7.5mg/mL BLf vs. 0.75mg/mL HA	****	-35.3%	< 0.0001
	0.45mg/mL HA vs. 0.75mg/mL HA	*	-17.0%	0.0111
60	2.5mg/mL BLf vs. 7.5mg/mL BLf	*	-16.2%	0.0195
	2.5mg/mL BLf vs. 0.45mg/mL HA	****	-23.3%	< 0.0001
	2.5mg/mL BLf vs. 0.75mg/mL HA	****	-33.6%	< 0.0001
	7.5mg/mL BLf vs. 0.75mg/mL HA	****	-20.7%	< 0.0001
	0.45mg/mL HA vs. 0.75mg/mL HA	*	-13.4%	0.0142
72	2.5mg/mL BLf vs. 0.45mg/mL HA	**	-17.4%	0.0013
	2.5mg/mL BLf vs. 0.75mg/mL HA	****	-22.6%	< 0.0001
	7.5mg/mL BLf vs. 0.75mg/mL HA	**	-14.5%	0.0056

With the control sample successfully growing, it was demonstrated that wounds supplemented with BLf were actually hindered in wound healing (Table 3). This was contrary to what was expected as both of the BLf concentrations in the scratch wound assay (Figure 25) closed more rapidly than that of the HA wounds. According to Ashby et al. [32], BLf does not improve proliferation of migration, but instead reduces the inflammation, thereby improving the wound

healing. This would explain why BLf influences a model with a higher inflammatory response (i.e. a more 'damaging' wound) such as scratch wound assay. As different cell types may respond differently to specific drugs, this could have also altered the results significantly [66]. The 0.75mg/mL HA significantly enhanced the HCEpC wound healing rate over the control at the 24, 48, 60 and 72-hour by 45%, 31%, 29% and 17%, respectively. Contradictory to what is expected, the 2.5mg/mL BLf decelerated the wound healing rate. This effect was significant showing a decrease in wound size by -27% at the 48-hour mark versus the control.

Table 3. Significance of BLf and HA on HCEpCs 2mm PDMS wound assay versus control

Time (h)	Sample	Significance	% improved	P-value
24	0.75mg/mL HA	**	45%	0.0082
48	2.5mg/mL BLf	***	-27%	0.0008
	0.75mg/mL HA	****	31%	<0.0001
60	0.75mg/mL HA	****	29%	<0.0001
72	0.75mg/mL HA	**	17%	0.0060

One issue while performing the PDMS wound assay was the weak adherence of the PDMS stamp to the surface of the well plate. Consideration to the rate at which media was added and removed is strongly suggested for future experiments. Additionally, any vibration in the surrounding area (i.e. opening and closing of the incubator) may trigger denuding of the PDMS stamp. It is also advised that transportation of the well plate between the incubator, microscope and bio-safety cabinet (BSC) should be performed as carefully and slowly as possible.

As the size of the wound was too large for a single image at the available 5X lens, no quantification was performed on initial wound size.

3.2.1.3 HCEpCs and RCEpCs 1mm PDMS wound assay

A 1mm PDMS wound assay experiment was employed using both HCEpCs and RCEpCs (Figure 29) to determine if PDMS wound assay could provide a more consistent initial wound area.

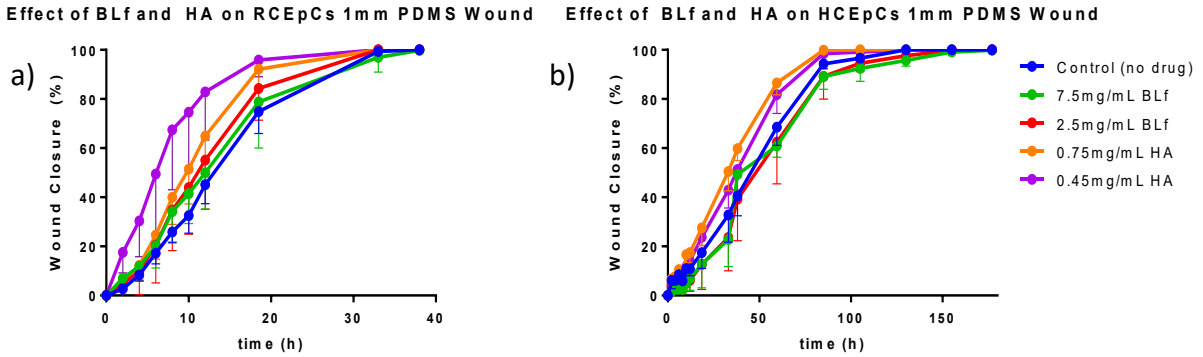

Figure 29. Effect of BLf and HA between RCEpC and HCEpC 1mm PDMS wound assays with a) n = 4 and b) (n = 5). Error bars shown are SD.

Most notably, the duration of wound healing between the two cell-types was distinct. The length of the HCEpCs wound assay was approximately one week, compared to that of the RCEpCs which healed within two days. This caused the percentage of accelerated rate of wound healing to be larger in the RCEpCs wound assay. Table 4 demonstrated the significance between the two drug types and concentrations on wound healing in an HCEpCs 1mm PDMS wound assay. It was demonstrated that the both the 2.5mg/mL and 7.5mg/mL BLf caused a significant decrease in wound healing compared to the 0.75mg/mL HA with the HCEpCs between the 10- and 85-hour. The difference between the two BLf concentrations were insignificant except at the 38-hour where a 7.5mg/mL BLf concentration allowed for a 25.8% decrease in wound size. The 7.5mg/mL BLf had a significantly larger wound area compared to the 0.45mg/mL HA between the 18.5-hour and 85-hour except at the 38-hour mark, with a 46.5% increase in wound area at the 18.5-hour and 9.5% by the 85-hour. The 2.5mg/mL BLf demonstrated a significantly reduced wound healing compared to the 0.45mg/mL HA from the 18.5-hour until the 85-hour.

Table 4. Significance between BLf and HA on HCEpCs 1mm PDMS wound assay

Time (h)	Samples	Significance	% improved	P-value
10	7.5mg/mL BLf VS 0.75mg/mL HA	**	-70.3%	0.0095
	2.5mg/mL BLf VS 0.75mg/mL HA	*	-61.7%	0.0303
12	7.5mg/mL BLf VS 0.75mg/mL HA	*	-59.7%	0.0267
	2.5mg/mL BLf vs. 0.75mg/mL HA	*	-65.0%	0.0128
18.5	7.5mg/mL BLf vs. 0.75mg/mL HA	***	-53.9%	0.0005
	7.5mg/mL BLf vs. 0.45mg/mL HA	**	-46.5%	0.0094
	2.5mg/mL BLf vs. 0.75mg/mL HA	***	-54.2%	0.0004
	2.5mg/mL BLf vs. 0.45mg/mL HA	**	-46.8%	0.0088
	7.5mg/mL BLf vs. 0.75mg/mL HA	****	-55.0%	<0.0001

33	7.5mg/mL BLf vs. 0.45mg/mL HA	****	-46.9%	<0.0001
	2.5mg/mL BLf vs. 0.75mg/mL HA	****	-53.1%	<0.0001
	2.5mg/mL BLf vs. 0.45mg/mL HA	****	-44.8%	<0.0001
38	7.5mg/mL BLf vs. 2.5mg/mL BLf	*	25.8%	0.0209
	7.5mg/mL BLf vs. 0.75mg/mL HA	*	-17.5%	0.0260
	2.5mg/mL BLf vs. 0.75mg/mL HA	****	-34.4%	<0.0001
	2.5mg/mL BLf vs. 0.45mg/mL HA	**	-23.5%	0.0035
59.5	7.5mg/mL BLf vs. 0.75mg/mL HA	****	-29.7%	<0.0001
	7.5mg/mL BLf vs. 0.45mg/mL HA	****	-25.6%	<0.0001
	2.5mg/mL BLf vs. 0.75mg/mL HA	****	-27.8%	<0.0001
	2.5mg/mL BLf vs. 0.45mg/mL HA	****	-23.6%	<0.0001
85	7.5mg/mL BLf vs. 0.75mg/mL HA	*	-10.7%	0.0209
	7.5mg/mL BLf vs. 0.45mg/mL HA	*	-9.5%	0.0393
	2.5mg/mL BLf vs. 0.75mg/mL HA	*	-10.7%	0.0222
	2.5mg/mL BLf vs. 0.45mg/mL HA	*	-9.4%	0.0417

The RCEpCs 1mm wound assay (Table 5) demonstrated similar results where the 2.5mg/mL and 7.5mg/mL BLf samples healed the wounds significantly slower than the 0.45mg/mL HA between the 6-12hour time points. Additionally, a higher concentration of 0.75mg/mL produced a slower wound healing from the 6-10hour.

Table 5. Significance between BLf and HA on RCEpCs 1mm PDMS wound assay

Time (h)	Samples	Significance	% improved	P-value
6	7.5mg/mL Blf vs. 0.45mg/mL HA	**	-59.2%	0.0045
	2.5mg/mL Blf vs. 0.45mg/mL HA	**	-58.4%	0.0052
	0.75mg/mL HA vs. 0.45mg/mL HA	*	-50.2%	0.0220
8	7.5mg/mL Blf vs. 0.45mg/mL HA	***	-49.5%	0.0009
	2.5mg/mL Blf vs. 0.45mg/mL HA	**	-48.5%	0.0011
	0.75mg/mL HA vs. 0.45mg/mL HA	**	40.8%	0.0086
10	7.5mg/mL Blf vs. 0.45mg/mL HA	***	-44.4%	0.0009
	2.5mg/mL Blf vs. 0.45mg/mL HA	**	-41.1%	0.0026
	0.75mg/mL HA vs. 0.45mg/mL HA	*	-31.0%	0.0374
12	7.5mg/mL BLf vs. 0.45mg/mL HA	**	-39.7%	0.0011
	2.5mg/mL Blf vs. 0.45mg/mL HA	**	-33.5%	0.0079

Although the means of both concentrations of either drug accelerated the wound healing of 1mm RCEpCs PDMS wound assay in Figure 29, it was calculated in

Table 6 that only the 0.45mg/mL HA and 0.75mg/mL HA had a significantly smaller wound area at various time points. The 0.45mg/mL HA was consistently significantly faster throughout the experiment, boasting a 149% increase in wound healing at the 4th hour which declined to 21% by the end of day one. A higher concentration of HA was less effective on the 1mm RCEpCs PDMS wound assay demonstrating a significant increase at the 12th hour of 35%. Both of the BLf concentrations tested did not significantly increase wound healing compared to the control (no additional drug), which was expected from the 2mm PDMS wound assay experiment.

Table 6. 1mm RCEpCs PDMS wound assay

Time (h)	Sample	Significance	% improved	P-value
4	0.45mg/mL HA	*	149%	0.0190
6	0.45mg/mL HA	***	103%	0.0002
8	0.45mg/mL HA	****	101%	< 0.0001
10	0.45mg/mL HA	****	81%	< 0.0001
12	0.75mg/mL HA	*	35%	0.0422
	0.45mg/mL HA	****	53%	< 0.0001
18.5	0.45mg/mL HA	*	21%	0.0277

The results shown in Table 7 show the 1mm PDMS wound assay using HCEpCs. A faster wound closure was established when supplemented with both concentrations of HA, whereas a detrimental rate occurred when BLf was added. The 2.5mg/mL and 7.5mg/mL BLf PDMS wound assays overall healed slower than the control, however, both concentrations were significantly slower at the 33rd hour by 33% and 40%, respectively. Additionally, the 7.5mg/mL BLf slowed the healing rate at the 38th hour by 37%. The 0.75mg/mL HA PDMS wound assay was revealed to be significant from the 18.5th hour until 59.5th hour beginning at a 58% increase to that of 26%. Similarly, the 0.45mg/mL HA sample demonstrated a significant accelerated wound healing from the 33rd hour until the 59.5th hour from 31% to 19% increase.

Table 7. 1mm HCEpCs PDMS wound assay

Time (h)	Sample	Significance	% improved	P-value
18.5	0.75mg/mL HA	*	58%	0.0179
33	7.5mg/mL BLf	*	-40%	0.0113
	2.5mg/mL BLf	*	-33%	0.0248
	0.75mg/mL HA	****	54%	< 0.0001
	0.45mg/mL HA	*	31%	0.0111
38	7.5mg/mL BLf	*	-37%	0.0320
	0.75mg/mL HA	****	48%	< 0.0001
	0.45mg/mL HA	**	27%	0.0056

59.5	0.75mg/mL HA	****	26%	< 0.0001
	0.45mg/mL HA	***	19%	0.0004

HA was selected as the molecule to be delivered using GelMA due to its consistency among cell types and wound types (scratch wound assay versus PDMS wound assay), ability to accelerate wound healing, lower concentration required to achieve the minimum effective concentration, and cost efficiency [67, 68].

This experiment also indicated a more consistent initial wound area with PDMS wound assay model. Among 23 selected samples, a 10.1% standard deviation in initial wound area was calculated using Graphpad Prism (Figure 30). The deviation could be due to variations in the 1mm punches from the elasticity of the GelMA. Few of the 1mm PDMS wound assays were damaged upon removal of the PDMS, however, these samples were not included in the calculation. The damage was caused by accidental scraping of the tweezers when uplifting the PDMS from the surface of the well plate (Figure 31). As the PDMS removal technique was easier to refine than the scratch wound while providing a wound size observable in a single image (providing an easier quantification with ImageJ software), a PDMS wound assay was chosen for future experiments.

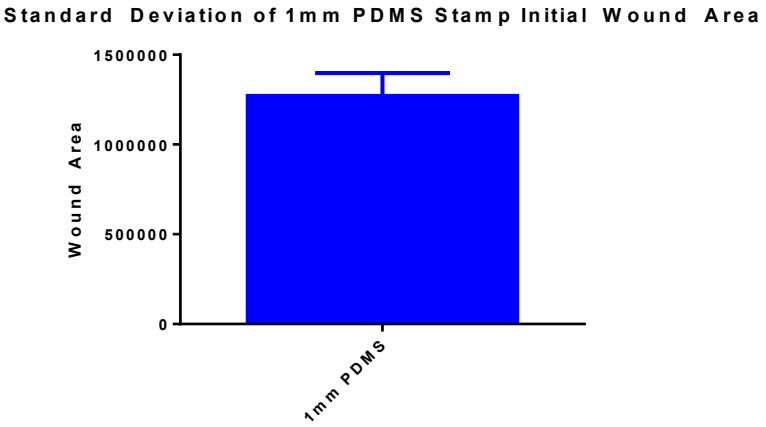

Figure 30. Standard deviation of initial wound area of 1mm PDMS wound assay (n =23). Error bar shown is SD.

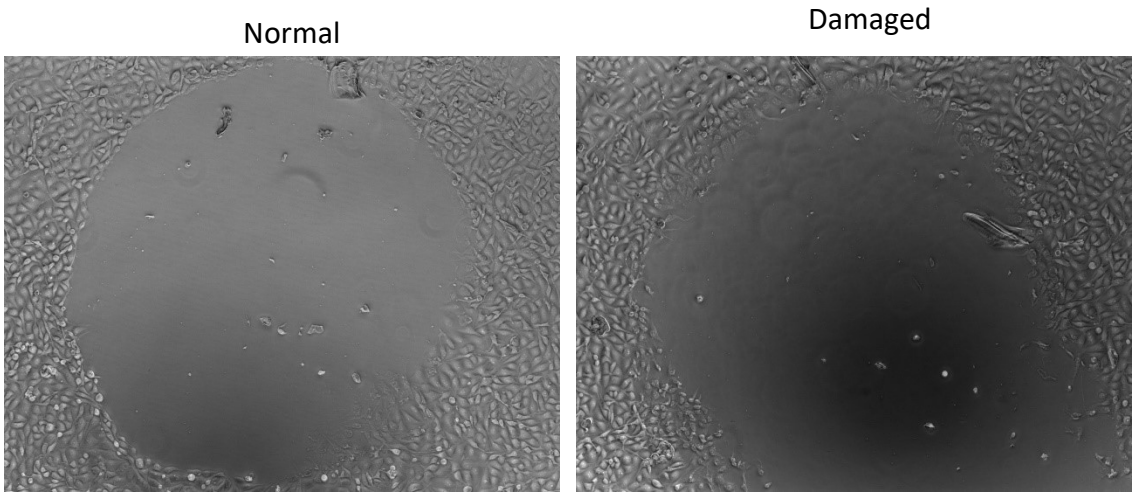

Figure 31. Phase contrast image of normal versus damaged 1mm PDMS initial wound area

3.2.2 HCEpCs Daily 60kDa

As the majority of literature assesses the effects of native HA (high molecular weight) and that of oligomer-HA (very low molecular weight) on epithelial wound healing [38, 39], this experiment was performed to determine the influence of mid-size (i.e. ~60kDa) HA on corneal wound healing. A PDMS wound assay with n = 5 was created using either 0.05, 0.1, 0.3, 0.6, or 1.0mg/mL of 60kDa HA (Figure 32). A 250ng/mL MMP-9 sample was included for reference to observe the effects of the enzyme on wound healing, similar to the MMP that would be present during the controlled release with GelMA.

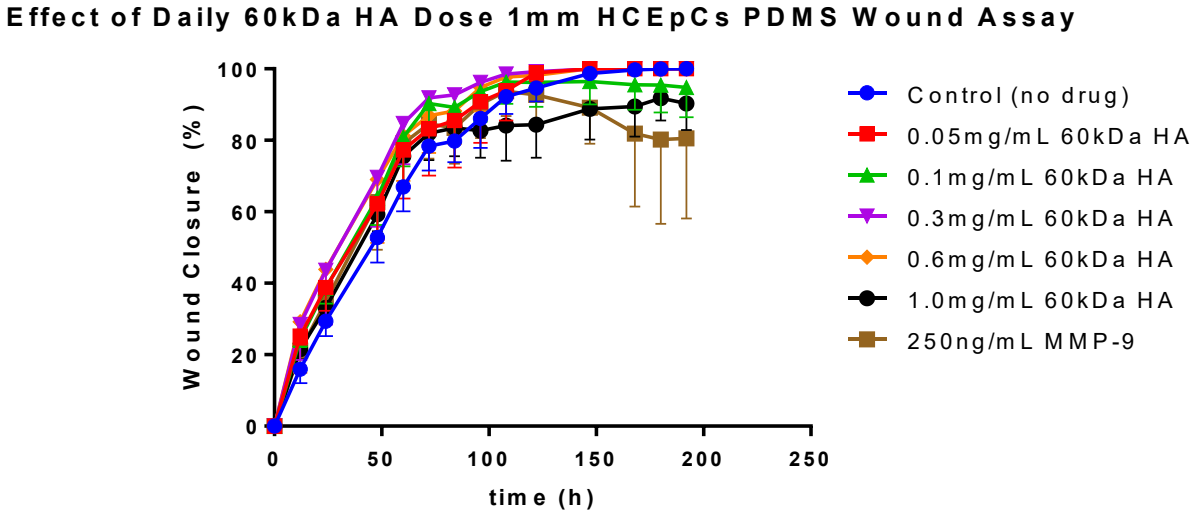

Figure 32. Daily 60kDa HA on 1mm HCEpC PDMS wound assay wound assay (n = 5). Error bars shown are SD.

The 0.3mg/mL, 0.6mg/mL and 0.05mg/mL HA-supplemented wounds healed more rapidly than the control, whereas the 0.1mg/mL and 1.0mg/mL HA samples had a detrimental effect. Table 8 demonstrates that at the 24, 48, and 60 hour time point, the 0.3mg/mL and 0.6mg/mL HA were significantly faster by 40% and 36% at 24 hours; 28% and 22% at 48 hours; and 24% and 18% at 60 hours, respectively. The 0.1mg/mL HA wound offered a significantly faster wound healing over the control by 15% at the 72 hour. The overall wound for the 0.05mg/mL, 0.3mg/mL and 0.6mg/mL HA samples healed 23.5%, 12.5% and 23.5% faster, respectively. The addition of MMP-9 initially had no effect on the wound healing, however, by day five, the wound expanded, causing a decrease in wound healing compared to the control, most significant at the 168, 180 and 192 hour by 19%, 21% and 21%, respectively. It is speculated that the delayed expansion of wound size can be interpreted similar to the closing of a drawstring bag. As the hole of the bag becomes smaller, the force pulling the strings must be higher to fully close the sack. Similarly, as the wound size decreases, the wound becomes more difficult to recover and therefore by day five, the MMP enzyme becomes an overburden and the wound expands.

Table 8. Daily 60kDa HA Addition on 1mm PDMS HCEpCs Wound Assay.

Time (h)	Sample	Significance	% improved	P-value
24	0.3mg/mL HA	*	40%	0.0369
	0.6mg/mL HA	*	36%	0.0324
48	0.3mg/mL HA	**	28%	0.0085
	0.6mg/mL HA	*	22%	0.0122
60	0.1mg/mL HA	*	21%	0.0434
	0.3mg/mL HA	**	24%	0.0047
	0.6mg/mL HA	*	18%	0.0345
168	250ng/mL MMP-9	**	-19%	0.0046
180	250ng/mL MMP-9	**	-21%	0.0013
192	250ng/mL MMP-9	**	-21%	0.0015

This experiment validated the use of a mid-size HA molecule in accelerating HCEpCs wound healing.

3.3 Controlled Release of 60kDa HA on 1mm HCEpCs PDMS wound assay

The information gathered in previous FITC-dextran controlled release experiments and the drug-supplemented PDMS wound assays investigations were combined to conduct this experiment. A larger 10H- GelMA patch of 8mm diameter was used in order to increase the amount of 60kDa that could be loaded. The 10H- GelMa patch was crosslinked using 600mW/cm^2 in order to

provide the highest amount of crosslinking possible and minimize the un-crosslinked material that may interfere. The KM media was changed at the previously mentioned time points and was stored in -80°C until a PDMS wound assay was prepared. This media containing 60kDa HA was utilized for both a wound assay to check the bioactivity as well as an ELISA to calculate a controlled release profile.

3.3.1 Bioactivity Assay

To test that the 60kDa HA was still bioactive upon release from a 10H- patch, the drug was subsequently delivered to a 1mm HCepCs PDMS wound assay. The 8mm patch either contained no drug (10H-) or was loaded with 150μg, 250 μg, 550 μg, or 750 μg 60kDa HA. Each GelMA sample was degraded using fresh 250ng/mL MMP-9 that was refreshed daily. A sample containing regular KM (control) and a sample with 250ng/mL MMP-9 in the media were also included. The data were graphed using GraphPad Prism as shown in Figure 33.

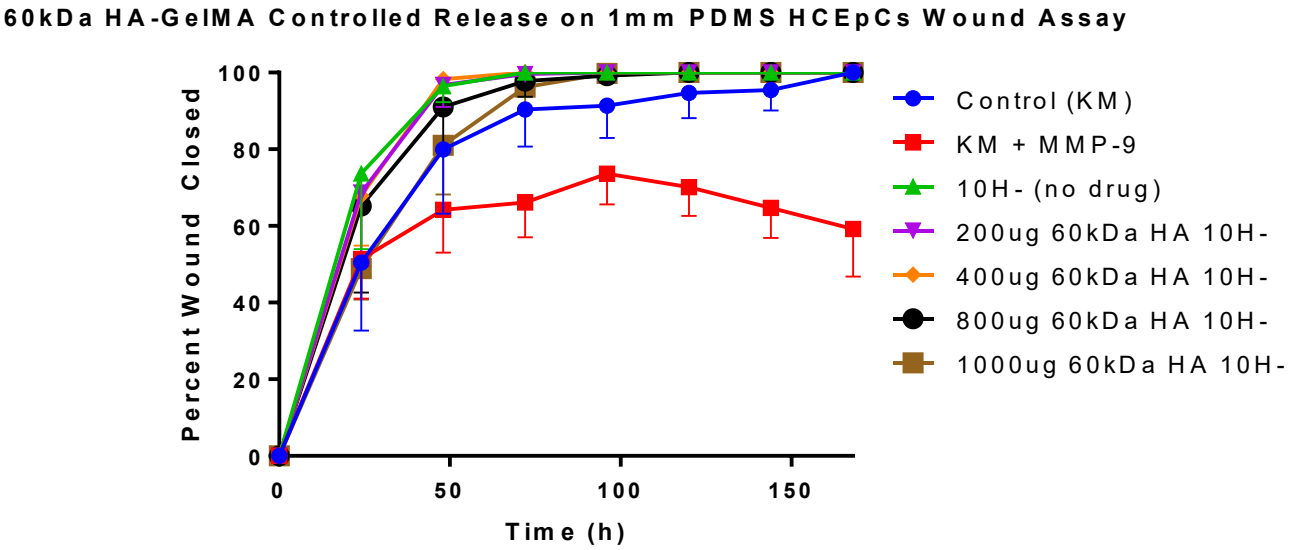

Figure 33. Controlled release of 60kDa HA from 10H- GelMA on 1mm HCEpCs PDMS wound assay Assay (n=4). Error bars shown are SD.

These results suggested that the degraded 10H- improved the wound healing rate of HCEpCs compared to a control (without MMP-9) in a 1mm PDMS wound assay model. This could be because GelMA is a conjugation of gelatin, a molecule known to aid in wound healing [70]. Additionally, gelatin coatings (containing a relatively low concentration of gelatin ~0.1%) [71] are a common supplement to aid in cell adhesion. Through this mechanism, the gelatin that is

degraded by the MMP-9 in KM solution may attach to the well plate surface to allow for the cells to rapidly migrate over the surface.

The addition of MMP-9 demonstrated a mean expansion in wound healing beginning at the 96-hour. This was as opposed to in Figure 32 where the enlarging of the wound did not occur until the 120-hour. This is speculated to be due to the previous experiment using a stock solution of 250ng/mL MMP-9 in KM media that was stored in the fridge, compared to this experiment where the MMP-9 was preserved in -80°C (along with each controlled release sample). The storage at -80°C could have preserved the bioactivity of the MMP-9 enzyme thereby causing an earlier onset of decreased wound area.

The 10H- sample revealed a significant improvement at the 24 and 48 hour mark by 37% and 16% over the control, respectively. Similarly, the 150μg and 250μg loaded-GelMAs displayed an accelerated wound healing at 24 hour mark of 28% and 26%; and the 48 hour mark of 16% and 18% increase, respectively. Lastly, although the mean of the 800μg loaded-GelMA sample overall healed slower than that of the 10H-, it was significantly faster than the control by 21% at the 24 hour mark.

Table 5. Significance of degradation of various 60kDa HA-loaded GelMA patches on 1mm PDMS HCEpCs wound assay compared to control

Time (h)	Sample	Significance	% improved	P-value
24	10H-	***	37%	0.0002
	150ug HA	**	28%	0.0056
	250ug HA	**	26%	0.0089
	550ug HA	*	21%	0.0376
48	10H-	*	16%	0.0146
	150ug HA	*	16%	0.0120
	250ug HA	**	18%	0.0051
	250ng/mL MMP-9	*	-24%	0.0227
72	250ng/mL MMP-9	****	-26%	< 0.0001
96	250ng/mL MMP-9	**	-18%	0.0075
120	250ng/mL MMP-9	****	-23%	< 0.0001
144	250ng/mL MMP-9	****	-27%	< 0.0001
168	250ng/mL MMP-9	****	-33%	< 0.0001

Comparing the HA-loaded samples to the bare 10H- that contained no drug, it was demonstrated that there was no significant improvement when incorporating the HA into the 10H- GelMA patch Table 9. One potential reason behind the insignificant increase in wound healing between the 10H- and the HA-incorporated GelMA patches could be due to the crosslinking of GelMA interfering with the bioactivity of HA. Alternatively, the amount of HA delivered daily may not have been sufficient to reach the minimum effective concentration (as discussed in section 3.3.2). It was additiionally demonstrated that the degradation of the $750\mu g$ 60kDa HA-loaded 10H- GelMA patch produced a significantly worse wound healing of -33.7% and -16.0% at the 24- and 48-hour, respectively, which suggested a concentration above the minimum toxic concentration.

Table 9. Significance of degradation of various 60kDa HA-loaded GelMA patches on 1mm PDMS HCEpCs wound assay compared to bare degraded 10H- GelMA patch

Time (h)	Sample	Significance	% improved	P-value
24	$750\mu g$ VS 10H-	****	-33.7%	< 0.0001
48	$750\mu g$ VS 10H-	**	-16.0%	0.0062

A vital observation that was made on the incorporation of HA into GelMA was that the GelMA precursor solution remained transparent upon complete dissolution of 60kDa HA, *however*, upon UV irradiation of the solution, the hydrogel became opaque white. This would pose a problem for a user as they would experience loss of vision. As the precursor solution remained transparent, it was thought that the dosage of HA was too high to be encapsulated with the crosslinking density of the GelMA, which would cause the HA to either precipitate out of solution [72] causing the material to become opaque. One potential solution to this is to select a different molecule that does not become opaque upon UV irradiation. Alternatively, an investigation of adhering GelMA to the conjunctiva can be implemented similar to muco-adhesive ocular drug delivery systems [73]. One such method is through the use of a methacrylated HA (HAMA)-GelMA hydrogel which has demonstrated a tunable swelling behaviour, mechanical properties and degradation rate [74].

3.3.2 ELISA of Controlled Release HA

$100\mu L$ of media that was used for the bioactivity assay was diluted to the appropriate linear range of the calibration curve given by the ELISA kit (50-1600ng/mL) [75]. This dilution was estimated based on the previous FITC-dextran controlled release experiments; an estimated 85% burst

release and 1.5% release rate over seven days. The accumulated release of 60kDa HA from the 10H- GelMA patch is illustrated in Figure 34.

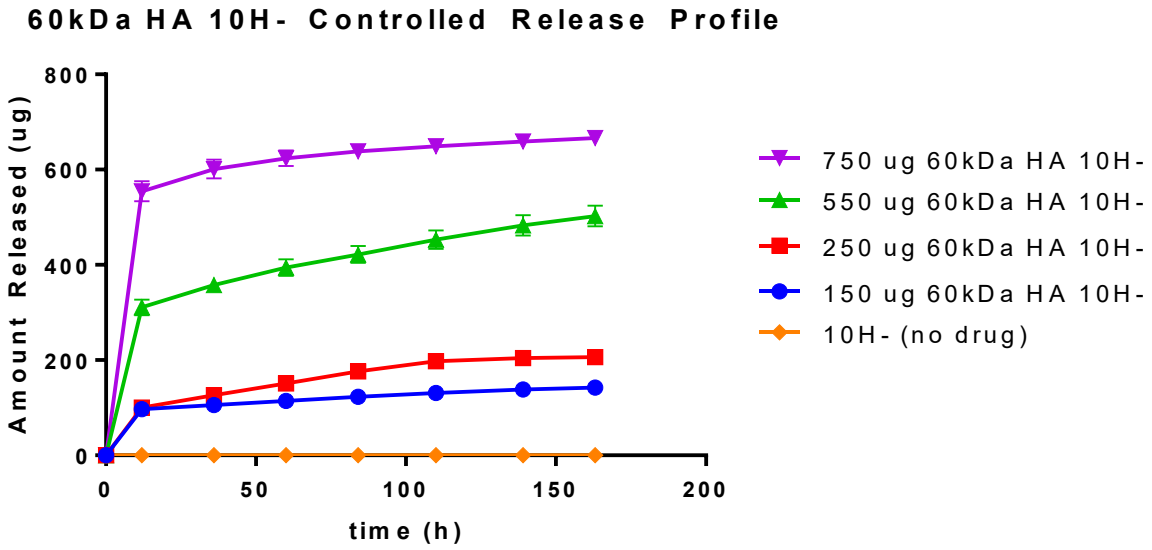

Figure 34. ELISA of 60kDa HA released from 10H- GelMA patch (n=2). Error bars shown are SD.

Each sample had a release profile similar to the previous 70kDa FITC-dextran release curves. The 750μg, 550μg, 250μg, and 150μg had a burst release of 83%, 62%, 49%, and 68%, respectively within the first 12 hours, with roughly a 5% daily release rate for the 150, 250, and 550μg samples and 2% for the 750μg samples. This low release rate may have been insufficient to reach a minimum effective concentration to improve the corneal epithelial wound healing compared to the bare 10H- degraded in 250ng/mL MMP-9. This could be verified by performing the controlled release experiment using multiple patches to obtain a higher amount of drug delivered. This option would prove to be more ideal over an increased loading due to the possibility of interference of HA during crosslinking.

The 10H- samples were fully degraded after the final time point and the percentage of drug that was loaded into the 10H- compared to the theoretical value for the 750μg, 550μg, 250μg, and 150μg samples were found to be 96%, 90%, 93% and 83%, respectively. The low loading into the 750μg sample could be due to a saturation of the solution, disallowing anymore drug to diffuse into the GelMA as the 750μg samples contained particles of 60kDa HA on the wound assay that were not fully dissolved (Figure 35), potentially residing on the outside of the 10H- patch. No such residue was found on 10H- samples loaded with a lower amount of 60kDa HA. Additionally,

the 750μg samples did not fully crosslink and consisted of a slimy texture. These results further suggest a phase separation occurred between the two polymers. This texture fragmented into the media as depicted by the floating particles in Figure 35. The presence of these particles could have hindered the ability of the cells to heal as shown in Table 9.

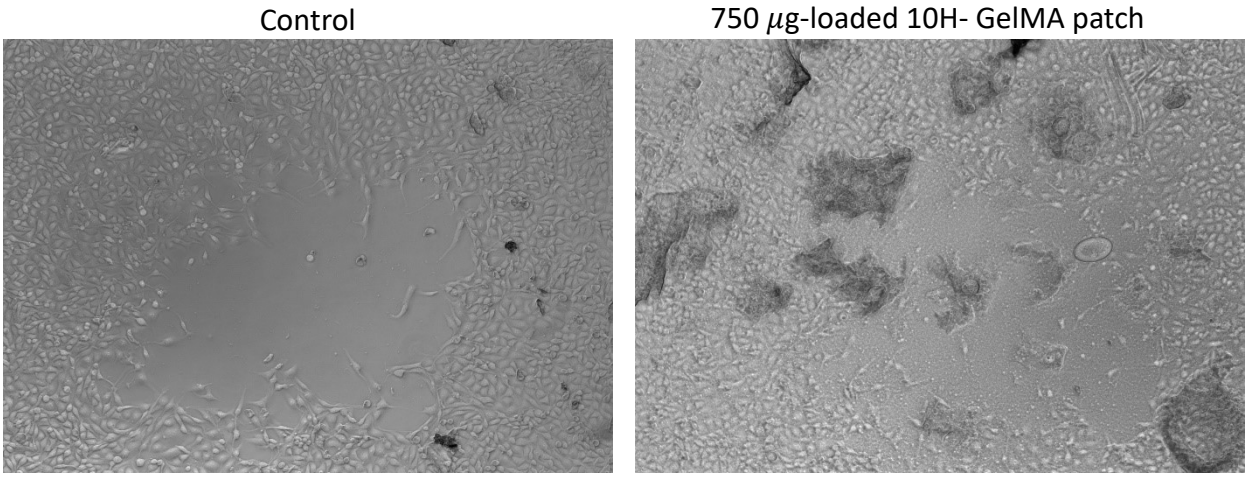

Figure 35. Residue from 750ug sample on surface of well plate on 1mm HCEpCs PDMS wound assay at t = 24

3.4 Application in Contact Lens

As the primary objective of this thesis was to aid in wound healing associated with RCE, it was initially envisioned that GelMA could be incorporated into pre-existing commercial CLs. It was later discovered that delivery through a GelMA patch provided a simpler production method as well as an unmatched drug loading to that of in CLs. Nonetheless, CLs did not demonstrate the ability to load a sufficient amount of drug (CL loaded below 10μg) to aid in our application. If another drug that possessed a lower minimum therapeutic concentration was discovered for ophthalmic purposes, CLs could potentially be used for this application. Although, insufficient for delivery of HA for RCE, CLs demonstrated great versatility as they were easily tuned through freeze-drying or patterning, among other methods.

3.4.1 Transmission, Wettability, Mechanical Strength Characterization

Arguably, the most important aspect of using a CL as a treatment method in the eye is that it remains completely transparent so the patient does not experience loss of vision. The CL mechanical properties should also not be compromised and more specifically, the surface properties remain similar. We have demonstrated that incorporation of GelMA into Biofinity CLs

lead to insignificant changes to the light transmission (in visible range), water contact angle measurements as well as mechanical strength as shown in Figure 36 and Figure 37.

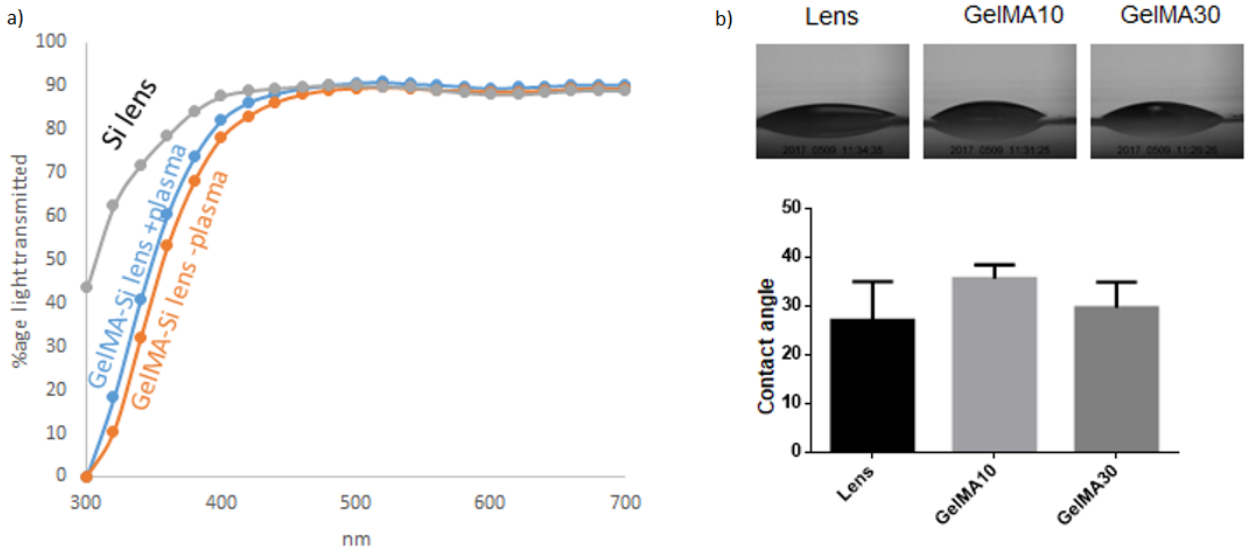

Figure 36. Effect of GelMA incorporation in commercial CL on a) light transmittance and b) surface wettability (n=3)

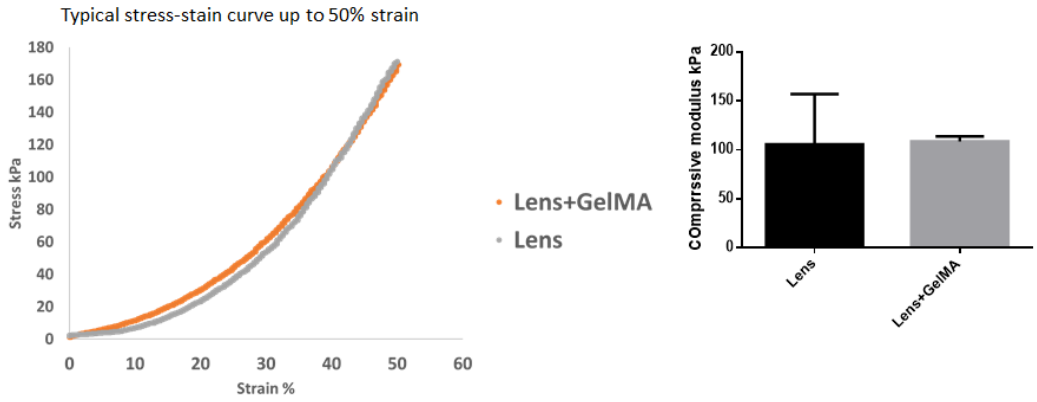

Figure 37. Effect of GelMA incorporation in commercial CL on stress-strain curve (n=3)

Neither 10% nor 30% GelMA altered the physical properties of the CL. Although there was a decrease in light transmittance from the 300-400nm range, the human eye is only able to see wavelengths between 390-700nm [76], and as such, there was no visible changes to the CL when viewing it with the naked eye. Additionally, no significant changes in water contact angle nor stress-strain curve for both the 10% and 30% GelMA were present. These results demonstrated that GelMA incorporated CLs is a viable option for delivering a low quantity of drug to the eye.

3.4.2 Optimization of GelMA incorporated CL

Experiments were performed in an attempt to optimize the controlled release profile of a 70kDa drug from a GelMA-incorporated CL. These investigations were aimed to improve the loading and controlled release profile of a GelMA-incorporated CL to be sufficient for an accelerated corneal epithelial wound healing. A design depicting the hypothesized mechanism is provided.

3.4.2.1 Drug Loading through Sonication (CL)

As the Biofinity Toric CLs do not possess a high volume of liquid (13.5-15.0mm in diameter and 0.08mm-0.60mm centre thickness [77]), the amount of drug that can be loaded is fractions to that of a GelMA patch. Optimization of drug loading in a CL was investigated by sonicating the lens to forcibly diffuse 70kDa FITC-dextran into the hydrogel matrix. This idea was based off of the concept of sonication increasing the pore size of dense nanofibers as demonstrated by Gu et al. [78].

A similar approach was employed to expand the CL hydrogel pores to load additional FITC-dextran prior to relaxation, thereby increasing encapsulation. Variations to the sequence of which the CLs were sonicated or soaked were tested. The samples were either sonicated in the GelMA solution prior to overnight soaking (SONON), sonicated immediately before UV crosslinking (ONSON), or sonicated in DI water followed by overnight soaking in GelMA (SONDION). The samples were then degraded overnight in $100\mu g/mL$ MMP-9 and the fluorescence was recorded (Figure 38).

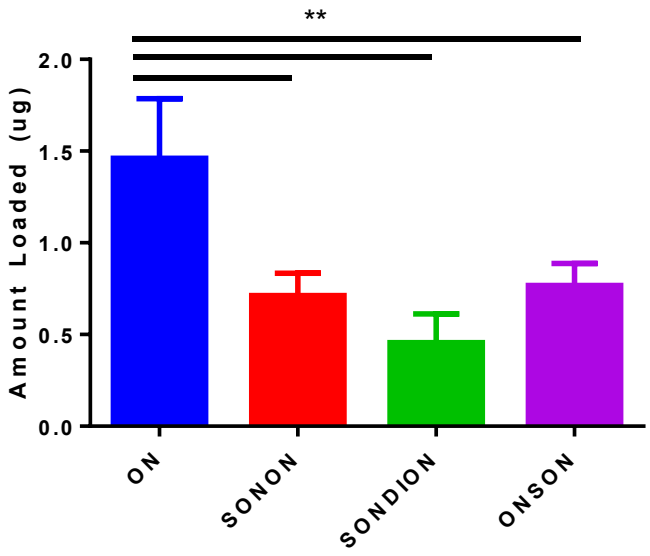

*Figure 38. Effect of sonication on drug loading in 10H- GelMA-incorporated contact lens (n=4). Error bars shown are SD. **: $p<0.005$*

Sonication decreased the amount of drug loaded, potentially due to drug being forced out of the contact lens during the sonication process. Alternatively, the relaxation time for the CL could have been longer than expected and the hydrogel may have been in an expanded form for an extended period of time, causing the drug to rapidly diffuse from the lens after crosslinking. This theory could be verified by examining the pore size using cryo-scanning electron microscope (cSEM) on a sonicated sample as described by Bodenberger et al. [79]. The lenses may additionally be examined in a controlled release experiment to observe the difference between slopes or burst release of the release profiles. A sonicated sample would expect to have a higher slope/burst release due to an expanded pore size.

3.4.2.2 Drug Loading through Freeze-Drying (CL)

Freeze-drying of the Biofinity CL was explored in order to remove remaining liquid that may exist within the hydrogel after overnight baking. This would theoretically grant a higher loading of drug as more space would be available to pack in the hydrogel. A diagram on the rationale behind this experiment is shown in Figure 39 and the results are shown in Figure 40.

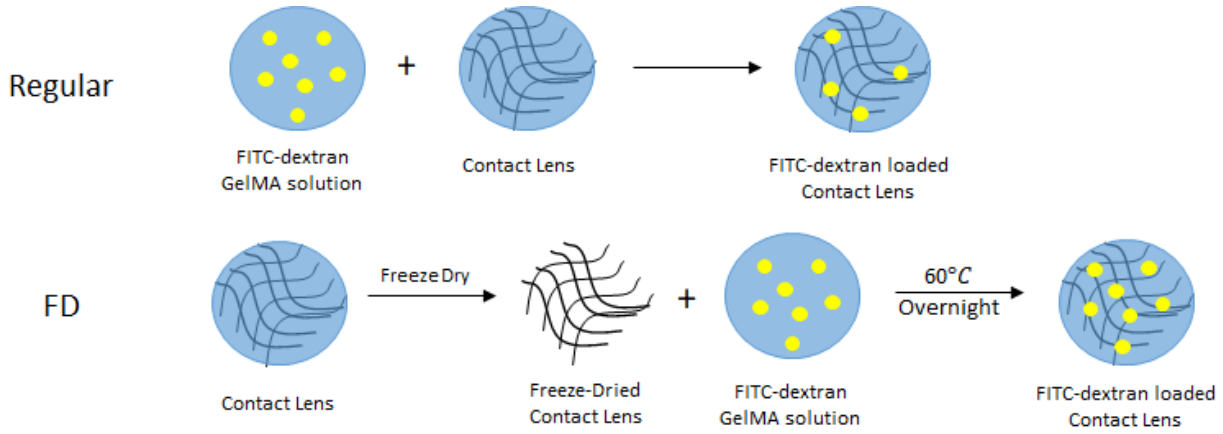

Figure 39. Schematic of proposed freeze drying method

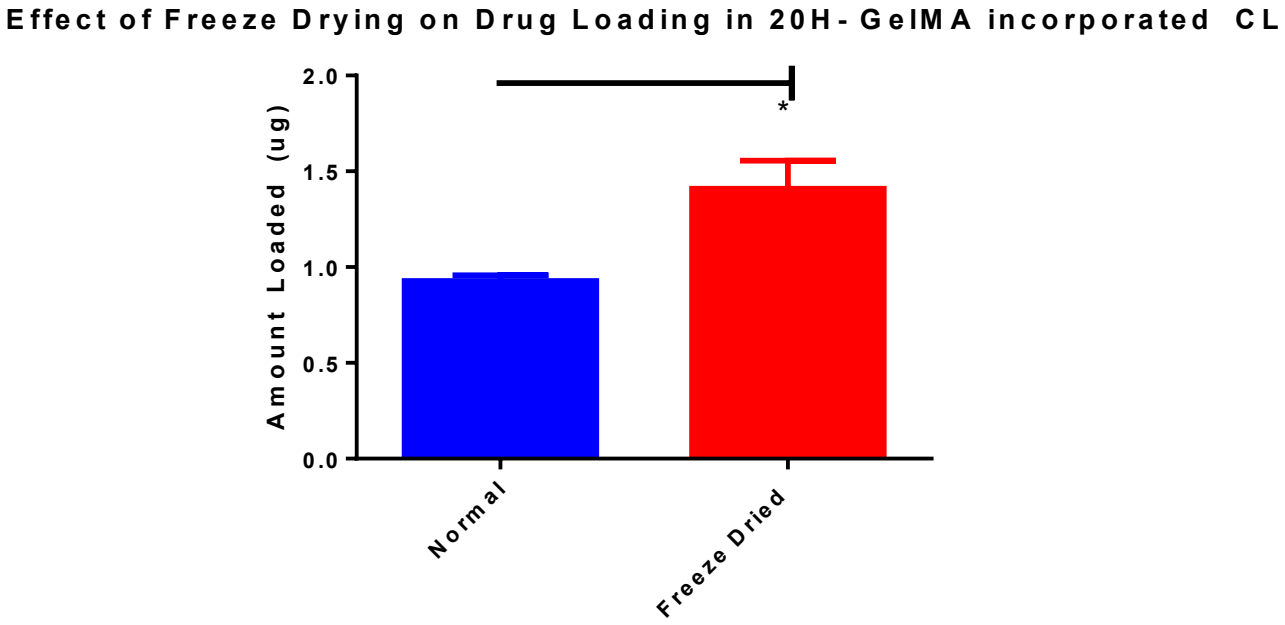

*Figure 40. Effect of freeze drying on drug loading in 10H-GelMA incorporated CL (n=3). Error bars shown are SD. *:p< 0.05*

A pre-freeze-drying step increased the FITC-dextran loading into CLs by ~50%. Increasing the volume of drug that soft CLs can load would be a top priority if the lens was the main transport vehicle. This would allow the CL to be used in a wider range of applications, however, as the amount loaded was still far too low for the molecules that were investigated for RCE, freeze-dried CLs were not used.

3.4.2.3 Contact Lens Extra Dipping

A proof of concept experiment was performed using a contact lens loaded with FITC-dextran and UV crosslinked. This lens was then dipped in a 20H- GelMA solution either with or without FITC-dextran and UV irradiated a second time. The rationale behind this method is depicted in Figure 41. By creating an external barrier to the FITC-dextran loaded GelMA-CL, the burst release would be minimized and a steadier release profile could be achieved. The barrier was provided as a means to provide a farther diffusion path and lower surface area for release to the external environment as well as slow the degradation by the MMP-9.

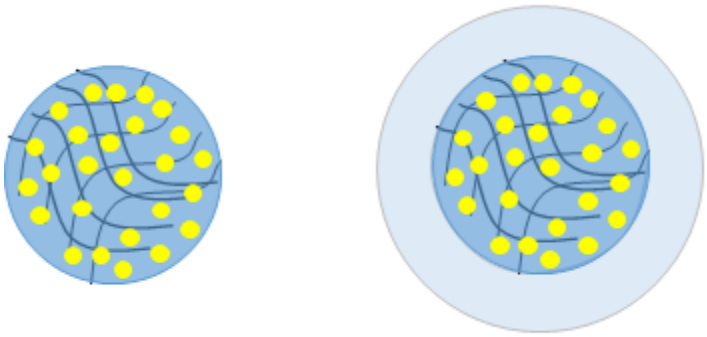

Figure 41. Schematic of proposed extra dipping mechanism

As UV irradiation of FITC-dextran quenches the fluorescence, a sample that was UV irradiated twice was included for comparison (Figure 42). It was also noted that a second dip of the contact lens would drastically alter the external properties and as such, this experiment was simply a proof of concept. The CL provided a physical material to dip twice (whereas the patch is fragile and may snap when picking up with tweezers) and for this reason, a CL was used to perform this experiment.

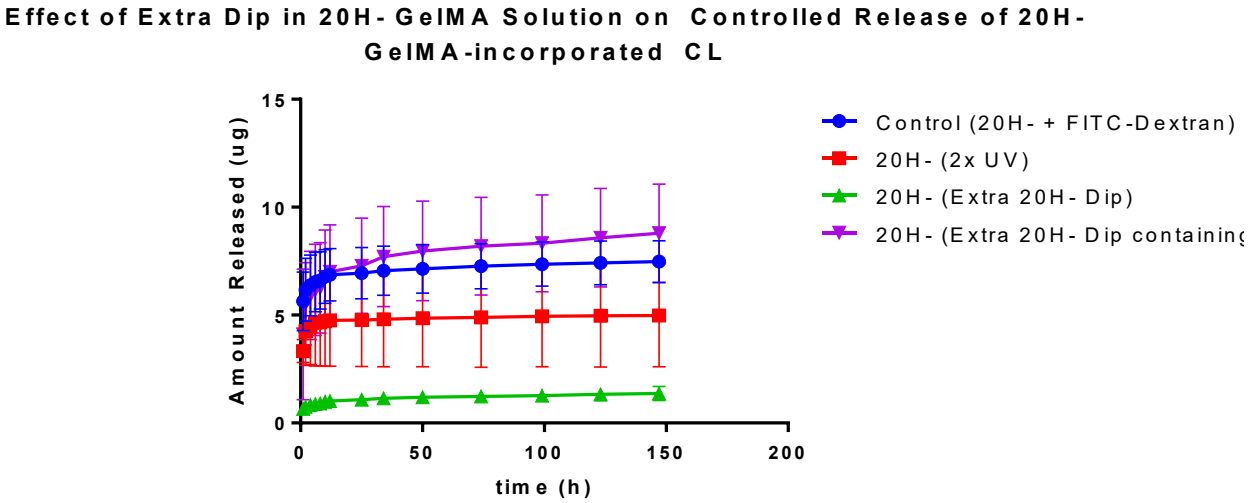

Figure 42. Effect of additional 20H- GelMA dipping on controlled release profile of 70kDa FITC-dextran from 20H-GelMA incorporated CL (n=3). Error bars shown are SD.

A second dip containing FITC-dextran provided a more sustained and higher release rate than that of the twice UV irradiated sample. This was expected as an additional amount of FITC was also added in the external barrier.

The sample containing an outer layer of bare 20H- GelMA appeared to have released a small amount of FITC-dextran. This could be due to an excessively thick outer layer preventing the FITC-dextran from diffusing through the barrier or, alternatively, the MMP-9 enzyme was not able to break down the barrier within seven days (a normal 20H- GelMA patch does not fully dissolve in 250ng/mL MMP-9 in a week time point). It is recommended that a lower concentration of GelMA (such as 10H-) should be attempted as an external barrier. If this proof of concept were to be explored further, it would be advised that a method to create a consistent thickness of barrier should also be investigated.

3.4.2.4 Alternate Interior Medium

The use of an alternate interior medium was used in an attempt to slow the burst release. PVA was added into the PBS solution to increase the viscosity of the solution thereby slowing the release of the FITC-dextran. A 20H- GelMA (control) was included for comparison (Figure 43).

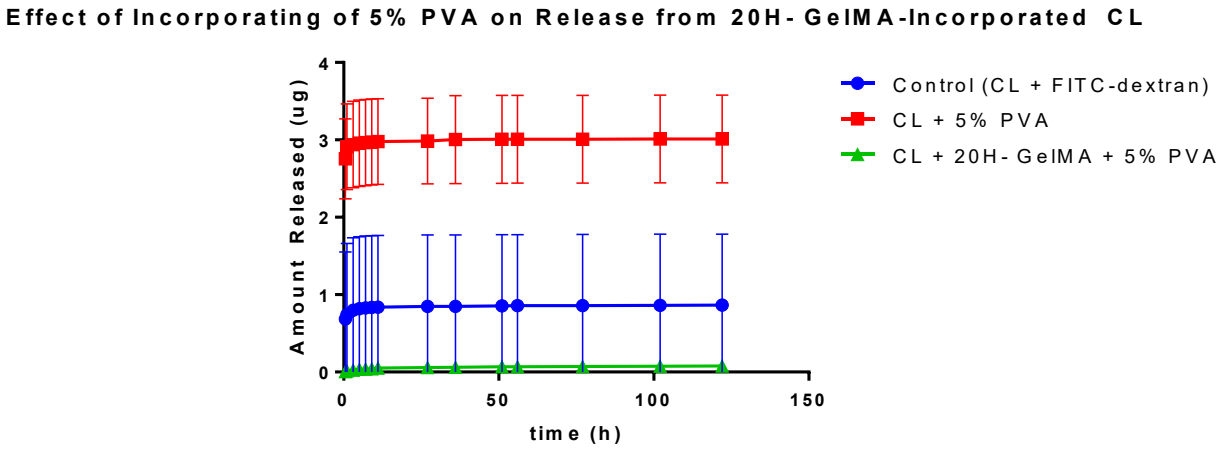

Figure 43. Effect of Alternate Interior Medium on Controlled Release of 70kDa FITC-dextran from 20H- GelMA-incorporated CL (n=3). Error bars shown are SD.

An alternate medium within the CL caused an increase burst release of FITC-dextran compared to both the control lens and the GelMA + 5% PVA sample. This increased burst release could be due to electrostatic interactions between the negatively charged PVA [80] and dextran polysaccharide. As GelMA is both negatively charged [81] and viscous, the combination may have forced the FITC-dextran out of the contact lens, thereby causing a low loading.

4. Conclusion and Recommendations

GelMA was investigated as a candidate for a controlled release material to the surface of the cornea for treatment of RCE syndrome. A tunable profile by altering the porosity, crosslinking site density, and permeability through the matrix was discovered through an additional physical crosslinking step, or adjustment of the methacrylation degree, concentration of GelMA and UV exposure time. A higher methacrylation degree and concentration of GelMA resulted in a more crosslinked gel and denser polymer matrix, respectively. These resulted in a lower burst release and stronger gel. The minimum UV dosage that was determined to create a 10H- GelMA patch capable of releasing drug over the course of seven days was 90,000 mJ/cm^2 at 365nm wavelength.

It was determined that a 4kDa FITC-dextran molecule was too small to be encapsulated in a GelMA hydrogel and was able to permeate freely throughout the gel resulting in a rapid elution and a diffusion-mediated release profile. The 70kDa FITC-dextran demonstrated a release profile dependant on the concentration of GelMA and additional crosslinking step, which increased the

density of polymer and decreased the pore size, respectively. It is recommended that a higher molecular weight molecule is tested with 30H+ GelMA to reduce the amount of diffusion-limited burst release and create a gel that is enzyme-mediated.

70kDa FITC-dextran model molecule was selected as the model molecule due to its cost efficiency and ease-to-quantify. It was discovered that FITC-dextran was sensitive to both the UV irradiation and the reagents incorporated to fabricate (GelMA precursor solution and IRGACURE 2959) and degrade (MMP-9) the GelMA patch. The amount of drug quantified after each controlled release experiment was lower than expected, accumulating only 1-60% of the theoretical amount of FITC-dextran loaded depending on the UV dosage. This decreased intensity was determined to be primarily due to dynamic quenching between the fluorophores and phase separation between the FITC-dextran and GelMA polymers. Regardless of the quenching, the FITC-dextran release profile accurately predicted the controlled release curve of 60kDa HA.

BLf and HA were shown to aid in corneal epithelial wound healing. It was speculated that BLf only accelerated wound healing by reducing the inflammatory response in cases such as in a scratch wound assay, and additionally showed significantly worse wound healing compared to the HA with the RCEpCs and HCEpCs. Conversely, 500kDa HA demonstrated more versatility, displaying an increased wound closure in both the scratch wound assay and PDMS wound assay models at the 0.45mg/mL and 0.75mg/mL concentrations. Due to its consistency and lower concentration requirements, HA was selected as the molecule to be loaded into a GelMA patch for a controlled release study on an HCEpCs PDMS wound assay. A 60kDa HA PDMS wound assay revealed a therapeutic range between 0.1-0.6mg/mL, increasing the wound healing rate by 40% in the first 24 hours, and by 24% in the 60^{th} hour.

A 10H-GelMA patch degraded in 250ng/mL MMP-9 demonstrated promising results 37% and 16% at the 24-hour and 48-hour mark, respectively. The incorporation of 60kDa HA into the GelMA patch did not demonstrate a significant increase in a 1mm HCEpCs wound assay. It is speculated that this is due to an insufficient amount of drug delivered to reach the minimum effective concentration. One vital issue that arose during the crosslinking of HA-loaded GelMA patches was the opaque gel that resulted which could have been due to phase separation between the HA

and GelMA. It is recommended that an HAMA-GelMA composite hydrogel is tested to remedy this issue.

As no consideration was taken into account for the friction caused from blinking. It is predicted future *in* vivo experiments would have a higher release rate due to the added stress on the hydrogel. To remedy this issue, a higher concentration of GelMA could be implemented for stronger mechanical properties and therefore a slower release rate. The effect of lipid and protein deposition were additionally not investigated on the drug release from a GelMA patch. It is recommended that the controlled release studies be performed in an artificial tear solution (to more closely mimic the *in vivo* environment) containing common tear film lipids (wax esters, cholesterols, fatty acids {Butovich, 2013 #321}). It is expected that the accumulation of lipids onto the surface of the GelMA patch may act as a physical diffusion-barrier that would reduce the release rate of drug similar to that observed with the incorporation of vitamin E {Shayani Rad M, 2017 #322}. Patterning of the hydrogels may also be incorporated to adjust for the decrease in release rate.

Although it was determined that CLs could not load a sufficient amount of drug to treat RCE with the selected molecules, the incorporation of GelMA into commercial CLs was also validated and optimized. It was found that CLs added further dimensionality to the controlled release profiles as they offered an additional freeze-drying and patterning step. Freeze-drying of the CL prior to soaking in GelMA allowed for an additional 50% of drug loaded. It was also discovered that the incorporation of GelMA did not significantly alter the physical properties of the CL such as its mechanical strength, light transmission in the visible range and the surface water contact angle. This revealed a potential for a variety of other ophthalmologic applications.

One controlled release method that was not pursued during this project was alternating charged layers on the CL for delivery. With the drug within one of the charged layers (either positive or negative – depending on the zeta potential of the drug), the electrostatic interactions between each layer will cause an impedance for a steady release [82]. This method was not investigated both due to time restraints as well as due to complications that may arise from alterations to the outside of the CL (difficult to incorporate into existing commercial products), however, if solutions to these problems are proposed, this method could be viable.

This project successfully put forth evidence validating a GelMA patch as a tunable controlled release material for the treatment of RCE. It is recommended that further investigation should be performed using either varying concentrations of HA or controlled release of multiple patches on a 1mm HCEpCs wound assay to determine if the minimum effective concentration was the cause of the insignificant increase wound healing and to investigate potential attachment of the patch to the conjunctiva. Nevertheless, the studies completed in this thesis demonstrated that a transparent, tunable GelMA material could have enormous implications in corneal drug delivery.

References

[1] R. Optical. (2018, 23 July). *Corneal Mapping*. Available: https://www.reedoptical.com/eye-care-services/corneal-mapping/

[2] A. A. o. Ophthalmology. (2018, 23 July). *Treatment of Recurrent Corneal Erosions*. Available: https://www.aao.org/eyenet/article/treatment-of-recurrent-corneal-erosions

[3] A. Golu, I. Gheorghisor, A. T. Balasoiu, F. Balta, E. Osiac, L. Mogoanta*, et al.*, "The effect of ultraviolet radiation on the cornea - experimental study," *Rom J Morphol Embryol,* vol. 54, pp. 1115-20, 2013.

[4] T. G. Rowsey and D. Karamichos, "The role of lipids in corneal diseases and dystrophies: a systematic review," *Clin Transl Med,* vol. 6, p. 30, Dec 2017.

[5] A. J. Rozsa and R. W. Beuerman, "Density and organization of free nerve endings in the corneal epithelium of the rabbit," *Pain,* vol. 14, pp. 105-20, Oct 1982.

[6] N. Efron, *Contact Lens Complications*: Saunders, 2012.

[7] R. R. Hodges and D. A. Dartt, "Tear film mucins: front line defenders of the ocular surface; comparison with airway and gastrointestinal tract mucins," *Exp Eye Res,* vol. 117, pp. 62-78, Dec 2013.

[8] M. D. P. Willcox, P. Argueso, G. A. Georgiev, J. M. Holopainen, G. W. Laurie, T. J. Millar*, et al.*, "TFOS DEWS II Tear Film Report," *Ocul Surf,* vol. 15, pp. 366-403, Jul 2017.

[9] J. Sowka, Gurwood, AS, Kabat, AG, *The Handbook of Ocular Disease Management*, 6 ed. vol. 150, 2013.

[10] E. J. H. W. Barry Lee, Mark Mannis, *Ocular Surface Disease: Cornea, Conjunctiva and Tear Film*, 2013.

[11] T. Sakimoto, J. Shoji, A. Yamada, and M. Sawa, "Upregulation of matrix metalloproteinase in tear fluid of patients with recurrent corneal erosion," *Jpn J Ophthalmol,* vol. 51, pp. 343-346, Sep-Oct 2007.

[12] S. J. Kridel, E. Chen, L. P. Kotra, E. W. Howard, S. Mobashery, and J. W. Smith, "Substrate hydrolysis by matrix metalloproteinase-9," *J Biol Chem,* vol. 276, pp. 20572-8, Jun 8 2001.

[13] N. L. Lanza, F. Valenzuela, V. L. Perez, and A. Galor, "The Matrix Metalloproteinase 9 Point-of-Care Test in Dry Eye," *Ocul Surf,* vol. 14, pp. 189-95, Apr 2016.

[14] D. Q. Li, B. L. Lokeshwar, A. Solomon, D. Monroy, Z. Ji, and S. C. Pflugfelder, "Regulation of MMP-9 production by human corneal epithelial cells," *Exp Eye Res,* vol. 73, pp. 449-59, Oct 2001.

[15] L. Sobrin, Z. Liu, D. C. Monroy, A. Solomon, M. G. Selzer, B. L. Lokeshwar*, et al.*, "Regulation of MMP-9 activity in human tear fluid and corneal epithelial culture supernatant," *Invest Ophthalmol Vis Sci,* vol. 41, pp. 1703-9, Jun 2000.

[16] S. Takeshita, T. Tokutomi, H. Kawase, K. Nakatani, H. Tsujimoto, Y. Kawamura*, et al.*, "Elevated serum levels of matrix metalloproteinase-9 (MMP-9) in Kawasaki disease," *Clin Exp Immunol,* vol. 125, pp. 340-4, Aug 2001.

[17] M. Schargus, S. Ivanova, V. Kakkassery, H. B. Dick, and S. Joachim, "Correlation of Tear Film Osmolarity and 2 Different MMP-9 Tests With Common Dry Eye Tests in a Cohort of Non-Dry Eye Patients," *Cornea,* vol. 34, pp. 739-44, Jul 2015.

[18] T. Sorensen and F. T. Jensen, "Tear flow in normal human eyes. Determination by means of radioisotope and gamma camera," *Acta Ophthalmol (Copenh),* vol. 57, pp. 564-81, Aug 1979.

[19] Y. Weng, J. Liu, S. Jin, W. Guo, X. Liang, and Z. Hu, "Nanotechnology-based strategies for treatment of ocular disease," *Acta Pharm Sin B,* vol. 7, pp. 281-291, May 2017.

[20] O. Aaron McNulty. (2018). *The OD's Guide to Managing Recurrent Corneal Erosion*. Available: https://www.reviewofoptometry.com/article/the-ods-guide-to-managing-recurrent-corneal-erosion

[21] S. S. Chaurasia, R. R. Lim, R. Lakshminarayanan, and R. R. Mohan, "Nanomedicine approaches for corneal diseases," *J Funct Biomater,* vol. 6, pp. 277-98, Apr 30 2015.

[22] H. Bahadar, F. Maqbool, K. Niaz, and M. Abdollahi, "Toxicity of Nanoparticles and an Overview of Current Experimental Models," *Iran Biomed J,* vol. 20, pp. 1-11, 2016.
[23] A. Patel, K. Cholkar, V. Agrahari, and A. K. Mitra, "Ocular drug delivery systems: An overview," *World J Pharmacol,* vol. 2, pp. 47-64, 2013.
[24] C. J. White and M. E. Byrne, "Molecularly imprinted therapeutic contact lenses," *Expert Opin Drug Deliv,* vol. 7, pp. 765-80, Jun 2010.
[25] A. F. Pimenta, A. P. Serro, P. Paradiso, B. Saramago, and R. Colaco, "Diffusion-Based Design of Multi-Layered Ophthalmic Lenses for Controlled Drug Release," *PLoS One,* vol. 11, p. e0167728, 2016.
[26] A. Hui, "Contact lenses for ophthalmic drug delivery," *Clin Exp Optom,* vol. 100, pp. 494-512, Sep 2017.
[27] A. V. Ljubimov and M. Saghizadeh, "Progress in corneal wound healing," *Prog Retin Eye Res,* vol. 49, pp. 17-45, Nov 2015.
[28] T. Kutila, S. Pyorala, H. Saloniemi, and L. Kaartinen, "Antibacterial effect of bovine lactoferrin against udder pathogens," *Acta Vet Scand,* vol. 44, pp. 35-42, 2003.
[29] L. Sanchez, M. Calvo, and J. H. Brock, "Biological role of lactoferrin," *Arch Dis Child,* vol. 67, pp. 657-61, May 1992.
[30] H. Wakabayashi, K. Yamauchi, and F. Abe, "Quality control of commercial bovine lactoferrin," *Biometals,* vol. 31, pp. 313-319, Jun 2018.
[31] S. Sharma, M. Sinha, S. Kaushik, P. Kaur, and T. P. Singh, "C-lobe of lactoferrin: the whole story of the half-molecule," *Biochem Res Int,* vol. 2013, p. 271641, 2013.
[32] B. Ashby, Q. Garrett, and M. Willcox, "Bovine lactoferrin structures promoting corneal epithelial wound healing in vitro," *Invest Ophthalmol Vis Sci,* vol. 52, pp. 2719-26, Apr 25 2011.
[33] U. Pattamatta, M. Willcox, F. Stapleton, N. Cole, and Q. Garrett, "Bovine lactoferrin stimulates human corneal epithelial alkali wound healing in vitro," *Invest Ophthalmol Vis Sci,* vol. 50, pp. 1636-43, Apr 2009.
[34] R. Stern, "Hyaluronan catabolism: a new metabolic pathway," *Eur J Cell Biol,* vol. 83, pp. 317-25, Aug 2004.
[35] Y. Akiyama, S. Jung, B. Salhia, S. Lee, S. Hubbard, M. Taylor*, et al.*, "Hyaluronate receptors mediating glioma cell migration and proliferation," *J Neurooncol,* vol. 53, pp. 115-27, Jun 2001.
[36] M. Nakamura, T. Nishida, M. Hikida, and T. Otori, "Combined effects of hyaluronan and fibronectin on corneal epithelial wound closure of rabbit in vivo," *Curr Eye Res,* vol. 13, pp. 385-8, May 1994.
[37] M. Nakamura, M. Hikida, and T. Nakano, "Concentration and molecular weight dependency of rabbit corneal epithelial wound healing on hyaluronan," *Curr Eye Res,* vol. 11, pp. 981-6, Oct 1992.
[38] M. Inoue and C. Katakami, "The effect of hyaluronic acid on corneal epithelial cell proliferation," *Invest Ophthalmol Vis Sci,* vol. 34, pp. 2313-5, Jun 1993.
[39] K. Ghazi, U. Deng-Pichon, J. M. Warnet, and P. Rat, "Hyaluronan fragments improve wound healing on in vitro cutaneous model through P2X7 purinoreceptor basal activation: role of molecular weight," *PLoS One,* vol. 7, p. e48351, 2012.
[40] A. B. C. Y. Leon Shargel, *Applied Biopharmaceutics & Pharmacokinetics*: McGraw-Hill Education, 2016.
[41] N. Mehrotra, M. Gupta, A. Kovar, and B. Meibohm, "The role of pharmacokinetics and pharmacodynamics in phosphodiesterase-5 inhibitor therapy," *Int J Impot Res,* vol. 19, pp. 253-64, May-Jun 2007.
[42] I. Advameg. (2018, 23 July). *How gelatin is made - production process, manufacture, making, used, processing, parts, structure*. Available: http://www.madehow.com/Volume-5/Gelatin.html
[43] M. Chaplin. (2018, 23 July). *Gelatin*. Available: http://www1.lsbu.ac.uk/water/gelatin.html
[44] J. W. Nichol, S. T. Koshy, H. Bae, C. M. Hwang, S. Yamanlar, and A. Khademhosseini, "Cell-laden microengineered gelatin methacrylate hydrogels," *Biomaterials,* vol. 31, pp. 5536-44, Jul 2010.

[45] K. Yue, G. Trujillo-de Santiago, M. M. Alvarez, A. Tamayol, N. Annabi, and A. Khademhosseini, "Synthesis, properties, and biomedical applications of gelatin methacryloyl (GelMA) hydrogels," *Biomaterials,* vol. 73, pp. 254-71, Dec 2015.
[46] D. M. H. Lee K. Fraiji, and T. C. Werner, "Static and dynamic fluorescence quenching experiments for the physical chemistry laboratory," *J. Chem. Educ.,* vol. 69, 1992.
[47] L. J.R., *Principles of Fluorescence Spectroscopy*: Springer, Boston, MA, 2006.
[48] A. Andersson, J. Danielsson, A. Graslund, and L. Maler, "Kinetic models for peptide-induced leakage from vesicles and cells," *Eur Biophys J,* vol. 36, pp. 621-35, Jul 2007.
[49] K. Schauenstein, E. Schauenstein, and G. Wick, "Fluorescence properties of free and protein bound fluorescein dyes. I. Macrospectrofluorometric measurements," *J Histochem Cytochem,* vol. 26, pp. 277-83, Apr 1978.
[50] B. H. Lee, N. Lum, L. Y. Seow, P. Q. Lim, and L. P. Tan, "Synthesis and Characterization of Types A and B Gelatin Methacryloyl for Bioink Applications," *Materials (Basel),* vol. 9, Sep 24 2016.
[51] P. M. RicardoCavicchioli, Khawar Sohail Siddiqui, TorstenThomas, "Proteins from Psychrophiles," *Methods in Microbiology,* vol. 35, pp. 395-436, 2006.
[52] T. Okada and Y. Ikada, "In vitro and in vivo digestion of collagen covalently immobilized onto the silicone surface," *J Biomed Mater Res,* vol. 26, pp. 1569-81, Dec 1992.
[53] U. Schroder, K. E. Arfors, and O. Tangen, "Stability of fluorescein labeled dextrans in vivo and in vitro," *Microvasc Res,* vol. 11, pp. 57-66, Jan 1976.
[54] G. K. Péter Veres, Gábor Nagy, István Lázár, István Fábián, József Kalmár, "Biocompatible silica-gelatin hybrid aerogels covalently labeled with fluorescein," *Journal of Non-Crystalline Solids,* vol. 473, pp. 17-25, 2017.
[55] D. Loessner, C. Meinert, E. Kaemmerer, L. C. Martine, K. Yue, P. A. Levett*, et al.*, "Functionalization, preparation and use of cell-laden gelatin methacryloyl-based hydrogels as modular tissue culture platforms," *Nat Protoc,* vol. 11, pp. 727-46, Apr 2016.
[56] M. W. Edelman, E. van der Linden, E. de Hoog, and R. H. Tromp, "Compatibility of gelatin and dextran in aqueous solution," *Biomacromolecules,* vol. 2, pp. 1148-54, Winter 2001.
[57] M. H.-B. Michael F Butler, "Phase separation in gelatin/dextran and gelatin/maltodextrin mixtures," *Food Hydrocolloids,* vol. 17, 2003.
[58] J. F. W. Alan J. Barrett, *Handbook of Proteolytic Enzymes*, 3rd ed.: Academic Press, 2013.
[59] B. Ratnikov, E. Deryugina, J. Leng, G. Marchenko, D. Dembrow, and A. Strongin, "Determination of matrix metalloproteinase activity using biotinylated gelatin," *Anal Biochem,* vol. 286, pp. 149-55, Nov 1 2000.
[60] M. Rizwan, G. S. L. Peh, H. P. Ang, N. C. Lwin, K. Adnan, J. S. Mehta*, et al.*, "Sequentially-crosslinked bioactive hydrogels as nano-patterned substrates with customizable stiffness and degradation for corneal tissue engineering applications," *Biomaterials,* vol. 120, pp. 139-154, Mar 2017.
[61] U. Eckhard, P. F. Huesgen, O. Schilling, C. L. Bellac, G. S. Butler, J. H. Cox*, et al.*, "Active site specificity profiling of the matrix metalloproteinase family: Proteomic identification of 4300 cleavage sites by nine MMPs explored with structural and synthetic peptide cleavage analyses," *Matrix Biol,* vol. 49, pp. 37-60, Jan 2016.
[62] V. A. Smith, H. Rishmawi, H. Hussein, and D. L. Easty, "Tear film MMP accumulation and corneal disease," *Br J Ophthalmol,* vol. 85, pp. 147-53, Feb 2001.
[63] A. Peer, R. Dhakal, R. Biswas, and J. Kim, "Nanoscale patterning of biopolymers for functional biosurfaces and controlled drug release," *Nanoscale,* vol. 8, pp. 18654-18664, Nov 10 2016.
[64] J. W.Gietzen, "Chapter 33 - Trauma-Oriented Ocular Examination, Corneal Abrasion, and Ocular Foreign Body Removal," in *Essential Clinical Procedures*, Second ed, 2007, pp. 453-470.
[65] L. Schneider, M. Cammer, J. Lehman, S. K. Nielsen, C. F. Guerra, I. R. Veland*, et al.*, "Directional cell migration and chemotaxis in wound healing response to PDGF-AA are coordinated by the primary cilium in fibroblasts," *Cell Physiol Biochem,* vol. 25, pp. 279-92, 2010.

[66] J. D. S. a. W. M. Reichert, "Chapter 1 Overview of Wound Healing in Different Tissue Types," in *Indwelling Neural Implants: Strategies for Contending with the In Vivo Environment.*, R. WM, Ed., ed: CRC Press/Taylor & Francis, 2008.

[67] S. Aldrich. (2018, 23 July). *Lactoferrin from bovine milk >=85% (SDS-PAGE)*. Available: https://www.sigmaaldrich.com/catalog/product/sigma/l9507?lang=en&region=CA

[68] L. Biomedical. (2018, 23 July). *Lifecore Biomedical Sodium Hyaluronate Pricing Guide*. Available: http://www.lifecore.com/sodium-hyaluronate/research-grade-sodium-hyaluronate/

[69] A. Jablonska-Trypuc, M. Matejczyk, and S. Rosochacki, "Matrix metalloproteinases (MMPs), the main extracellular matrix (ECM) enzymes in collagen degradation, as a target for anticancer drugs," *J Enzyme Inhib Med Chem,* vol. 31, pp. 177-183, 2016.

[70] J. M. M. I. Shukanta Bhowmik, Tonmoy Debnath, Muhammed Yusuf Miah, Shovon Bhattacharjee and Mubarak A. Khan, "Reinforcement of Gelatin-Based Nanofilled Polymer Biocomposite by Crystalline Cellulose from Cotton for Advanced Wound Dressing Applications," *Polymers,* vol. 9, 2017.

[71] R. Haas, S. S. Banerji, and L. A. Culp, "Adhesion site composition of murine fibroblasts cultured on gelatin-coated substrata," *J Cell Physiol,* vol. 120, pp. 117-25, Aug 1984.

[72] X. Huang and C. S. Brazel, "On the importance and mechanisms of burst release in matrix-controlled drug delivery systems," *J Control Release,* vol. 73, pp. 121-36, Jun 15 2001.

[73] B. M. Boddupalli, Z. N. Mohammed, R. A. Nath, and D. Banji, "Mucoadhesive drug delivery system: An overview," *J Adv Pharm Technol Res,* vol. 1, pp. 381-7, Oct 2010.

[74] G. Camci-Unal, D. Cuttica, N. Annabi, D. Demarchi, and A. Khademhosseini, "Synthesis and characterization of hybrid hyaluronic acid-gelatin hydrogels," *Biomacromolecules,* vol. 14, pp. 1085-92, Apr 8 2013.

[75] E. B. Inc. (2018, 23 July). *Hyaluronan Enzyme-Linked Immunosorbent Assay (HA ELISA)*. Available: http://www.echelon-inc.com/index.php?module=Products&func=detail&id=230

[76] C. M. C. Wei Teng Neo, Zugui Shi, Soo-Jin Chua and Jianwei Xu, "Modulating high-energy visible light absorption to attain neutral-state black electrochromic polymers," *Journal of Materials Chemistry C,* vol. 4, pp. 28-32, 2016.

[77] BIOFINITY. (2014, 23 July). *BIOFINITY (comfilcon A) Soft (Hydrophilic) Contact Lenses For Planned Replacement* Available: https://coopervision.com/sites/default/files/LF0125A_Package%20Insert_comfilcon%20A_Biofinity_Sphere%20Toric%20Multifocal.pdf

[78] S. J. P. Bon Kang Gu, Eun Sun Lee, Min Sup Kim, Yong Jin Lee and Chun-Ho Kim, "Beneficial effect on hemostatic function of blended chitosan/gelatin nanofiber mat with enhanced porosity using ultra-sonication," in *10th World Biomaterials Congress*, Montreal, 2016.

[79] D. K. Nicholas Bodenberger, Irina Abrosimova, Annika Scharm, Franziska Kipper, Paul Walther, Frank Rosenau, "Evaluation of methods for pore generation and their influence on physio-chemical properties of a protein based hydrogel," *Biotechnology Reports,* vol. 12, pp. 6-12, 2016.

[80] V. B. M. Wiśniewska, I. Ostolska, K. Szewczuk-Karpisz, K. Terpiłowski, A. Nosal-Wiercińska, "Impact of poly(vinyl alcohol) adsorption on the surface characteristics of mixed oxide Mn x O y –SiO2," *Adsorption,* vol. 22, pp. 417-423, 2015.

[81] G. B. M. R. Kadri, A. Tamayol, B. Aliakbarian, H. Y. Zhang, M. Hasan, L. Sánchez-González and E. Arab-Tehrany, "Preparation and characterization of nanofunctionalized alginate/methacrylated gelatin hybrid hydrogels" *RSC Advances,* 2016.

[82] J. Junthip, N. Tabary, F. Chai, L. Leclercq, M. Maton, F. Cazaux*, et al.*, "Layer-by-layer coating of textile with two oppositely charged cyclodextrin polyelectrolytes for extended drug delivery," *J Biomed Mater Res A,* vol. 104, pp. 1408-24, Jun 2016.